EP 2012-02

# Assessment of the potential for pelitic-mafic-type volcanogenic massive sulphide mineralization in the Labrador Trough

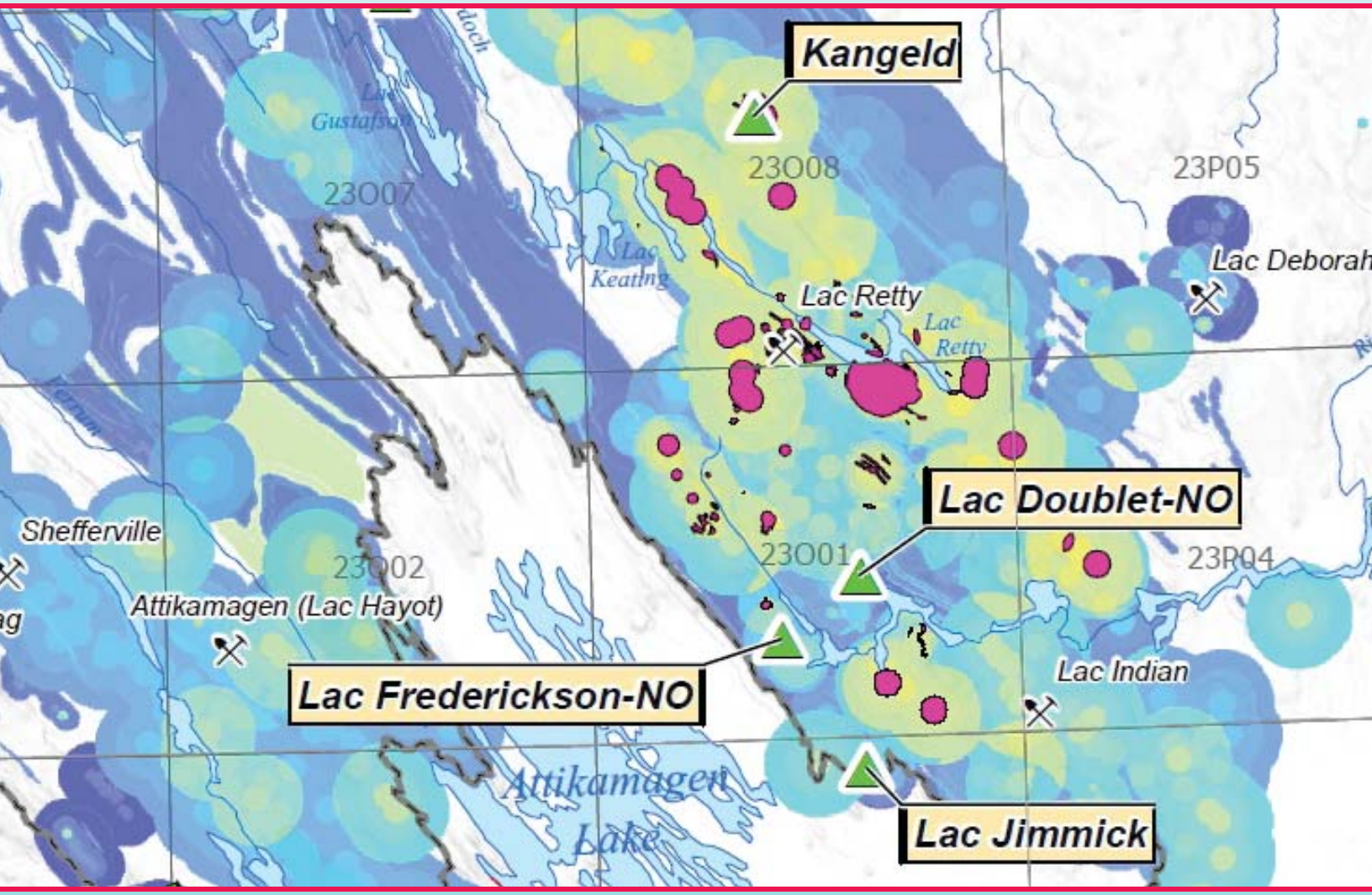


**Daniel Lamothe**

**2013**

Québec

DOCUMENT PUBLISHED BY GÉOLOGIE QUÉBEC

**Direction générale de Géologie Québec**
Robert Giguère, par intérim

**Direction de l'information géologique**
Luc Charbonneau, par intérim

**Service de la diffusion et de l'intégration**
Jean-Yves Labbé, par intérim

**Bureau de l'exploration géologique**
Patrice Roy, par intérim

**Editing**
Charles Gosselin

**Translation**
Venetia Bodycomb

**Graphic Design**
André Tremblay

Document accepted for publication on May 02, 2013

Dépôt légal - Bibliothèque et Archives nationale du Québec, 2013
ISBN : 978-2-550-68116-8

## Summary

The Labrador Trough contains several sizeable volcanogenic massive sulphide deposits of the pelitic-mafic (Besshi) type. Formed in volcano-sedimentary environments, deposits of this type are characterized by grades of roughly 3 to 5% Cu+Zn and tonnages that may exceed 100 Mt (Windy Craggy, Ducktown). The two largest deposits in the study region are Soucy-1 (5.44 Mt at 1.49% Cu, 1.80% Zn, 1.61 g/t Au, 13.7 g/t Ag) and Prud'homme-1 (5.31 Mt at 1.57% Cu, 1.36 Zn, 1.37 g/t Au and 21.9 g/t Ag). Both are located in the northern part of the Trough, but several other deposits are found in the southern part (Lac Murdoch-West, Lac Frederickson-NW).

This mineral potential assessment aims to outline zones in the Labrador Trough that are favourable for the discovery of new volcanogenic massive sulphide mineralization of the pelitic-mafic type. Data processing involved the weighting and combination of 25 geological parameters considered relevant to this type of mineralization in order to generate a predictive mineral potential map. The weight of each parameter was calculated according to its spatial association with known deposits of the target type, and the parameters were combined using a fuzzy logic approach. Favourable zones were created by choosing a significant threshold from among the fuzzy values of the resultant map.

Data modelling was done using the ModelBuilder tool in ArcGIS 9.3. The ability to quickly test new parameters or different calibration sets represents a significant improvement to the mineral potential assessment process. Most of the operations use original (unmodified) tables from the SIGEOM database as their source. This approach makes it possible to easily regenerate a new mineral potential map following updates to SIGEOM that affect the source data for the model.

# TABLE OF CONTENTS

# INTRODUCTION

The advent of GIS (Geographic Information System) platforms in the early 1990s led to the development of various approaches to process and combine multiple geological parameters in order to define favourable zones for the exploration of economic commodities (Chung and Agterberg, 1980; Bonham-Carter *et al.,* 1988; Harris, 1989; Agterberg *et al.* 1990; Chung and Moon, 1991; Bonham-Carter, 1994; Rencz *et al.,* 1994; Harris *et al.,* 1995; Wright and Bonham-Carter, 1996; Singer and Kouda, 1997a and b; Raines, 1999; Harris *et al.,* 2001; Brown *et al.,* 2000; D'Ercole *et al.*, 2000; de Araujo and Macedo, 2002; Porwal *et al.,* 2003a and b). Many potential assessment studies based on georeferenced data integration were also published for various metallogenic models, namely:

- volcanogenic massive sulphide (VMS) deposits (Wright and Bonham-Carter, 1996; Dion and Lamothe, 2002; Lamothe *et al.*, 2005; Lamothe, 2011);
- orogenic gold deposits (Groves *et al.*, 2000; Knox-Robinson, 2000; Harris *et al.*, 2001; Rogge *et al*., 2006; Lamothe and Harris, 2006; Lamothe, 2008)
- epithermal gold deposits (Boleneus *et al.*, 2001);
- Mississippi Valley deposits (D'Ercole *et al.*, 2000);
- Olympic Dam-Kiruna-type deposits (Lamothe and Beaumier, 2001 et 2002);
- kimberlite potential (Labbé, 2002; Paganelli *et al.*, 2002; Wilkinson *et al.*, 2006);
- porphyry Cu-Au±Mo deposits (Carranza and Hale, 2002; Tangestani and Moore, 2003; Labbé, *et al*., 2006, Lamothe, 2009).

The production of a mineral potential map involves a series of steps (Figure 1). First, an appropriate exploration model (VMS, orogenic gold, etc.) must be selected for the targeted commodity or commodities. Based on the model, relevant geological parameters are selected and combined to create a **favourability** map. This initial step is crucial because it allows the modeller to assess the availability of georeferenced data sources for each parameter and, if necessary, to determine the

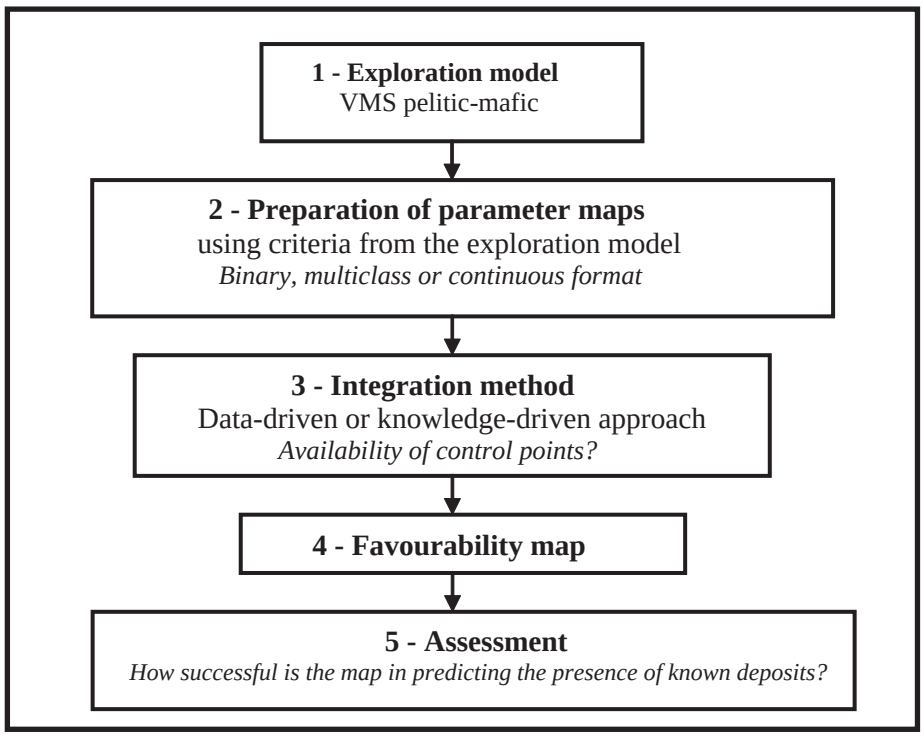


**FIGURE 1** – Steps to create a favourability map through georeferenced data integration (modified from Harris and Sanborn-Barrie, 2006).

amount of time needed to acquire new sources of data. It is also during this step that an appropriate geodesic reference system and map projection will be chosen.

The second step consists of generating, for each selected parameter, a **parameter map** that will be integrated when processing the exploration model. The format of each map may be either binary (0 or 1), multiclass or continuous (Harris *et al.*, 1999, 2000 and 2001). This step generally requires the use of spatial analysis or statistical processing programs, often available as GIS extensions.

The third step of processing is to integrate the various parameter maps to produce a favourability map. Integration methods are subdivided into two categories (Table 1): empirical or data-driven methods and conceptual or knowledge-driven methods (see Bonham-Carter, 1994 and Wright and Bonham-Carter, 1996 for a detailed description). Empirical approaches require the presence, within the study area, of a sufficient number of mineralized examples belonging to the targeted deposit model. These methods analyze spatial correlations between specific geological parameters and the location of known mineralization, thus allowing a weight to be assigned to each parameter. Processing methods such as the Weights of Evidence method (WofE; Bonham-Carter, 1994), logistic regression (Chung and Agterberg, 1980) and neural network analysis (Singer and Kouda, 1996 and 1999; Harris and Pan, 1999; Brown *et al.*, 2000) are all examples of this type of data-driven approach (Table 1).

Conceptual approaches rely on the modeller's expertise to assign a weight to each parameter based on the exploration model. Although subjective, these methods make it possible to integrate the geologist's knowledge and experience in the modelling process. These methods include Boolean logic, index overlay (Harris, 1989), the Dempster-Shafer belief theory (Chung and Moon, 1991; An *et al.*, 1992) and fuzzy logic (An *et al.*, 1991).

It is possible to combine the two types of approaches and develop hybrid methods. For example, to assess the mineral potential for SEDEX-type deposits in India (Porwal *et al.*, 2003b) and VMS-type or orogenic gold deposits in the Abitibi and James Bay region (Lamothe *et al.*, 2005; Lamothe and Harris, 2006; Lamothe, 2008, 2011), these authors used the WofE method to assign weights to the parameters, then converted these values into fuzzy weights and combined the parameter maps using fuzzy logic (this is also the approach used in the present study). In another example, Brown *et al.* (2003) used parameter maps weighted by fuzzy logic and combined them using neural networks to assess the mineral potential for orogenic gold deposits in Western Australia.

**TABLE 1** – Methods to integrate parameter maps in a GIS environment.

| Method | Processing | Combination criteria |
|---|---|---|
| **Data-driven methods** | | |
| Weights of evidence (WofE) | Control points (known deposits or occurrences) | Establish spatial correlations between known occurrences and tested variables (using Bayes' probability theorem) |
| Logistic regression | Control points (known deposits or occurrences) | Use spatial zones around known deposits to determine statistical criteria to apply to data layers in order to predict the presence or absence of mineral deposits |
| Neural networks | Control points (known deposits or occurrences) | Reproduce an anomalous set (i.e., mineral deposits) through a shape-recognition process |
| **Knowledge-driven methods** | | |
| Boolean operations | Geologist input | Sum of binary maps |
| Index overlay | Geologist input | Sum of weighted binary maps |
| Inference network and decision tree used in an expert system | Geologist input | |
| Dempster Shafer belief theory | Geologist input | |
| Fuzzy logic | Geologist input | Assign to each indicator element map a fuzzy weight factor between 0 and 1; combine maps using fuzzy operators (and, or, gamma) |
| Analytic hierarchy process (AHP) | Geologist input | Sum of weighted favourability (continuous maps) |

Favourability studies produced by the MRNF (Lamothe, 2008, 2011; Lamothe and Harris, 2006; Labbé *et al.*, 2006; Lamothe *et al.*, 2005) diverge from the vast majority of other mineral potential assessment studies in two key aspects: 1) high-favourability zones (HFZs) are defined through the objective determination of a minimum favourability threshold; and 2) **targets** are defined based on unstaked portions of the HFZs at the time of the study (see the section titled "Determination of high-favourability zones").

The end result of the integration process is a georeferenced mineral potential map illustrating high-favourability zones for the targeted commodity. In addition to adequately predicting the presence of known deposits, this map should also reveal the existence of new exploration areas.

The purpose of this study is to determine the location of high-favourability zones for pelitic-mafic-type VMS deposits in the Labrador Trough (Figure 2).

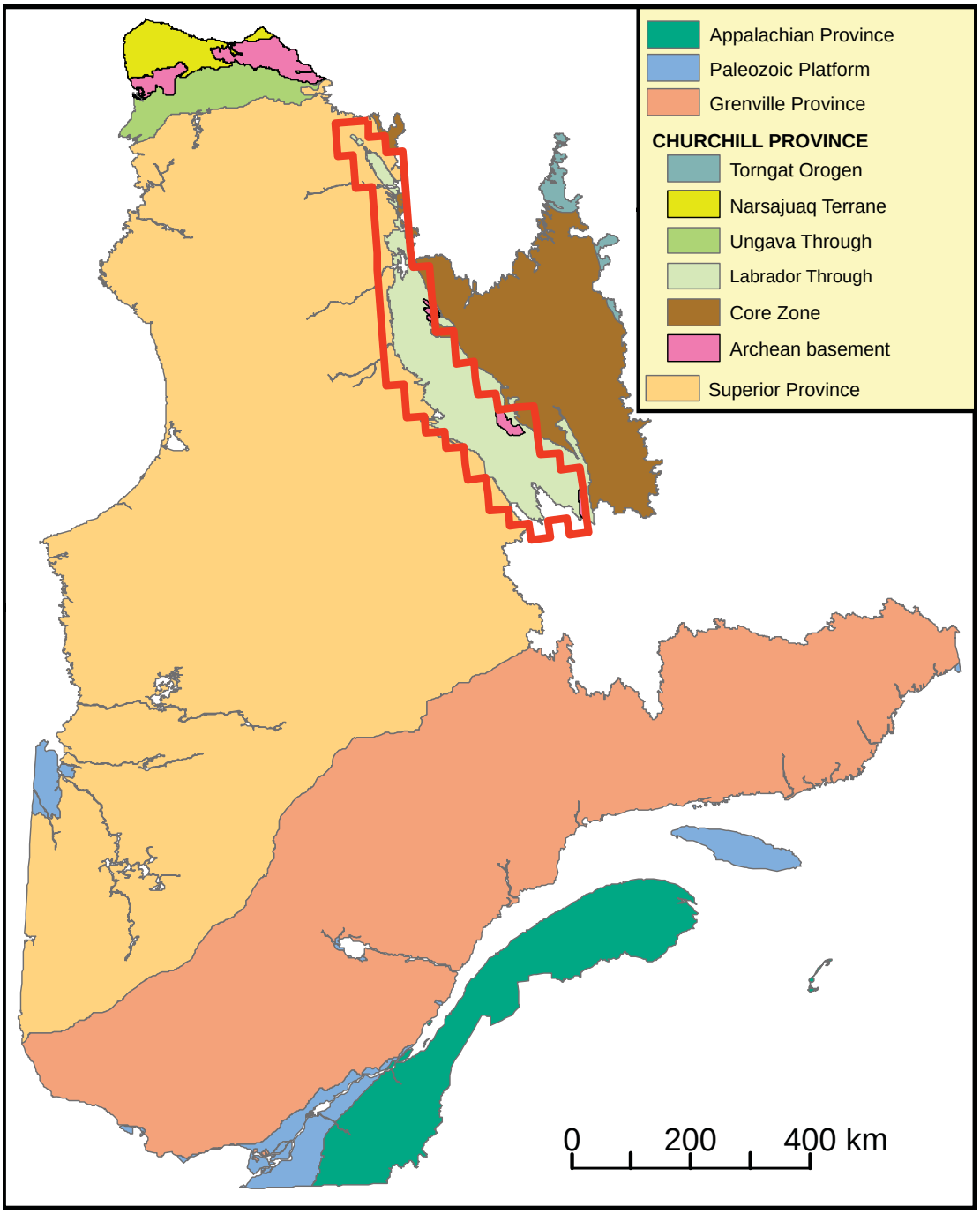


**FIGURE 2** – Location of the study region.

## General geology

The Labrador Trough constitutes the western part of the New Québec Orogen (Hoffman, 1988), which is located east of the Archean Superior Province and is part of the Circum-Ungava Geosyncline. Together, the Circum-Ungava Geosyncline and the Ungava Orogen border the northeast edge of the Superior Province in Québec (Figure 2; Dimroth *et al*., 1970; Baragar and Scoates, 1981). The Labrador Trough comprises autochthonous/parautochthonous belts of Paleoproterozoic supracrustal rocks (2.17– 1.87 Ga; Stockwell, 1982; Machado *et al.*, 1989; Clark and Thorpe, 1990; Machado, 1990; Rohon *et al.*, 1993; Skulsky *et al.*, 1993; Machado *et al.*, 1997). In the east, the orogen also contains an internal metamorphic-plutonic zone, known as the Core Zone, formed largely of Archean rocks (Figure 2; Wardle *et al.*, 2002; Hoffman, 1988; Poirier *et al.*, 1990; van der Leeden *et al.*, 1990; Wardle *et al.*, 1990a, 1990b, 2002; Girard, 1990; James and Dunning, 2000).

Supracrustal rocks constitute the Kaniapiskau Supergoup (Frarey and Duffell, 1964), which was subdivided by Clark and Wares (2004) into eleven lithotectonic zones (Figure 3). This assemblage forms a large synclinorium attributed to the oblique dextral collision between the Archean internal zone of the orogen, to the east, and the Superior Province, to the west (Hoffman, 1989, 1990; Wardle *et al.*, 1990b, 2002).

## Stratigraphy

The Kaniapiskau Supergroup comprises three main volcano-sedimentary cycles deposited over a period of about 300 Ma (Figure 4). The rocks of the first cycle (2169 – *ca* 1940 Ma, Clark and Thorpe, 1990) unconformably overlie the Superior craton and begin with a continental rift sequence of immature sandstone and conglomerate belonging to the Seward Group, followed by sandstones and dolomites of the Pistolet Group that were deposited in a passive continental margin setting. Platform subsidence led to the development of a basin and the deposition of Swampy Bay Group basalts and flyschs. The first cycle ended with the deposition of the Attikamagen Group, consisting of a platformal dolomitic reef complex signaling marine regression (Hoffman and Grotzinger, 1989).

The second cycle (1880 to 1870 Ma) began with a transgressive sequence of platform sediments unconformably overlying Archean basement and rocks of the first cycle. In the northern part of the orogen, this sequence is composed of the Ferriman Group which correlates chronostratigraphically with the volcano-sedimentary Doublet, Koksoak and Le Moyne groups deposited in a basin further to the east, in the south-central and southern parts of the Trough (Clark and Wares, 2004). Progressive deepening of this basin at the end of the second cycle is marked by the appearance of voluminous basaltic volcanism (Hellancourt Formation) and by the deposition of distal flyschs (Lower and Upper Baby formations).

The deposition of rocks belonging to the second cycle is associated with the emplacement of numerous mafic-ultramafic sills of tholeiitic affinity ("Montagnais sills" of Clark and Wares, 2004). These sills are contemporaneous and comagmatic with spatially-associated volcanic rocks (St. Seymour *et al.*, 1991; Rohon *et al.*, 1993; Skulski *et al.*, 1993; Findlay *et al.*, 1995). A major carbonatite intrusion (Le Moyne intrusion; Birkett and Clark, 1991) was emplaced in the summital part of the sequence towards the end of the second cycle.

The third sedimentary cycle, deposited *ca* 1.8 Ga (Clark and Wares, 2004) along an unconformity over rocks of the second cycle, consists of synorogenic molasses belonging to the Chioak Formation to the north and the Tamarack River Formation to the south.

## Characteristics of pelitic-mafic-type VMS deposits

The general class of volcanogenic massive sulphide (VMS) deposits is characterized by accumulations of massive sulphides in volcanic or volcano-sedimentary rocks. These deposits almost always form in a seafloor setting. They commonly originate from the concentrated circulation of near-surface hydrothermal fluids (Figure 5) and belong to the general class of exhalative deposits, which also includes SEDEX-type sedimentary exhalative deposits (Eckstrand *et al*., 1996). The VMS classification of Franklin *et al*. (2005), which is based on dominant host rocks lithologies and was adopted for this study, recognizes five categories of VMS deposits: 1) bimodal-mafic; 2) dominantly mafic; 3) pelitic-mafic; 4) bimodal-felsic; and 5) siliciclastic-felsic.

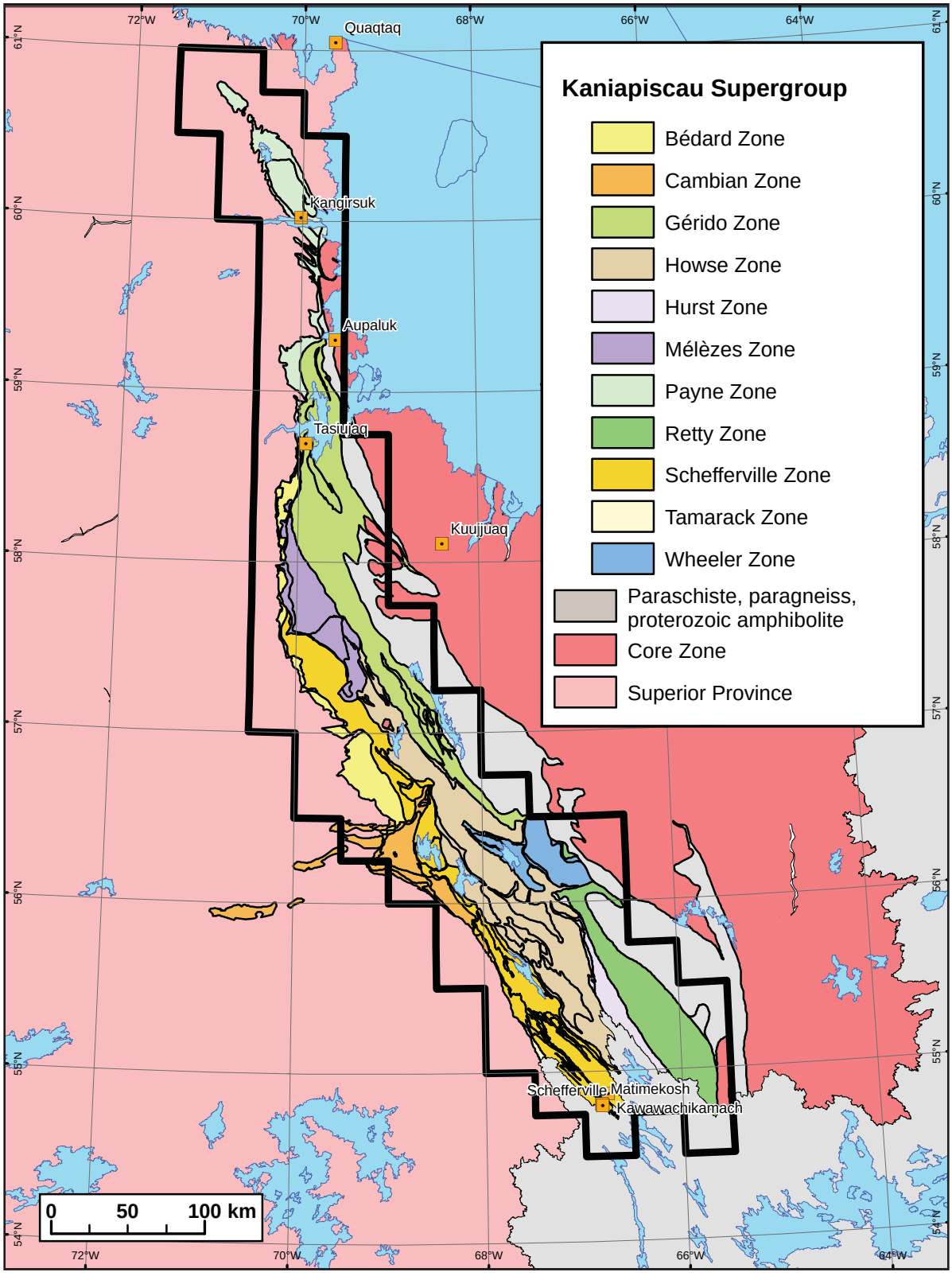


**FIGURE 3** – General geology of the Labrador Trough according to Clark and Wares (2004). The lithotectonic zones (see legend) are characterized by lithological assemblages or a coherent internal structural style and are bounded by tectonic discontinuities. The black outline represents the limit of the mineral potential assessment zone.

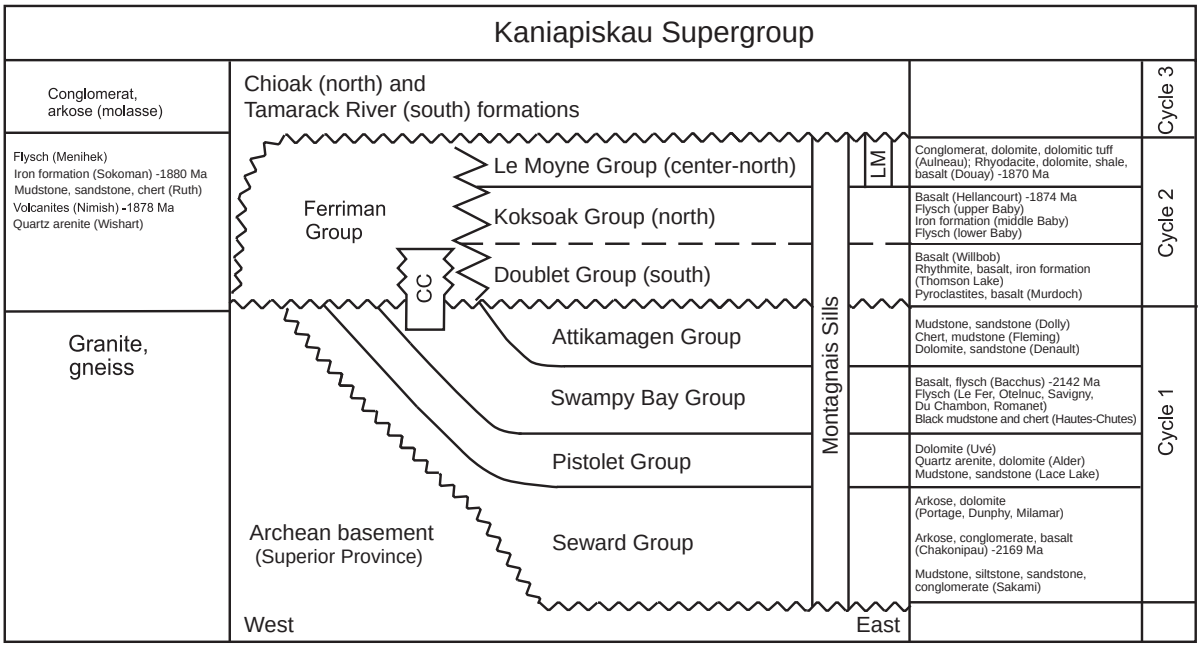


**FIGURE 4** – Schematic stratigraphy of the three cycles in the foreland of the New Québec Orogen (Clark and Wares, 2004). In this new interpretation, all groups constituting the three cycles belong to the Kaniapiscau Supergroup. The Sakami Formation correlates with the Seward Group and is grouped with this unit in the figure.

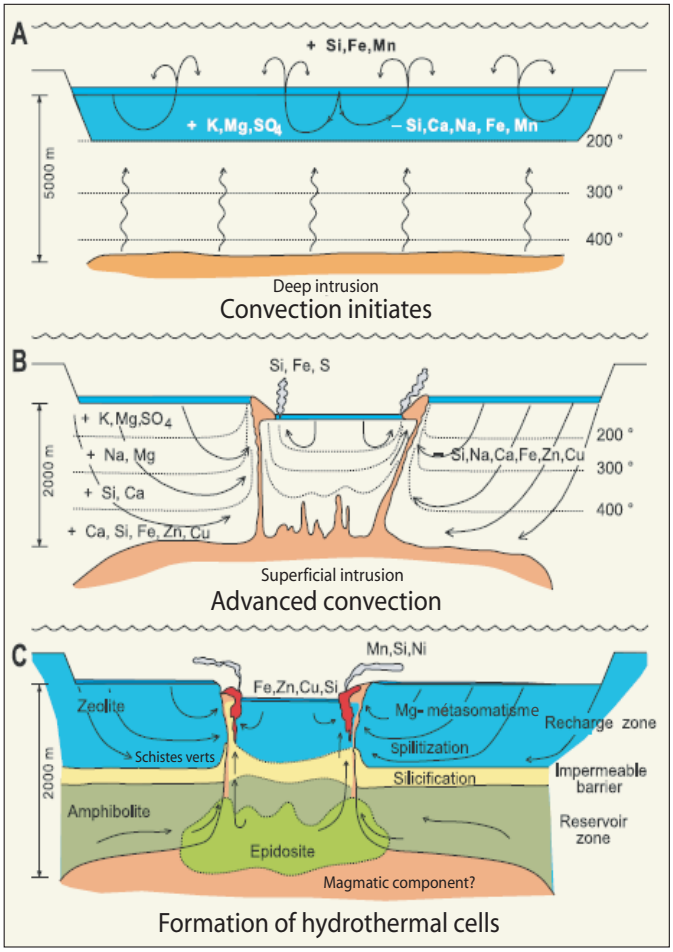


**FIGURE 5** – General model of the formation of VMS deposits (modified from Galley *et al.*, 2007)

The VMS deposit type modelled for the current study belongs to the pelitic-mafic category, also known as Besshi-type. These deposits are characterized by concordant, massive stratiform mineralization composed primarily of sphalerite, chalcopyrite, pyrrhotite and pyrite. Mineralization, exhalative in origin and associated with local hydrothermal activity, is syngenetically emplaced in a volcano-sedimentary assemblage of basalt and pelites deposited in a back-arc basin or mid-ocean ridge environment (Franklin *et al*., 2005). The best known example is Windy Craggy (>210 Mt at 1.66% Cu, 0.09% Co, 3.5 g/t Ag and 0.2 g/t Au) in British Columbia. A modern equivalent of this type of deposit is Bent Hill, which is found along the Middle Valley transform fault north of the Juan de Fuca ridge, alongside Vancouver Island (Figure 6; GSC website, 2008). The most significant characteristics of pelitic-mafic-type VMS deposits are listed in Table 2.

The size of pelitic-mafic-type VMS deposits varies from less than 1 Mt to greater than 300 Mt, with grades between 0.64% and 3.3% Cu (Franklin *et al*., 2005). Figure 7 illustrates the metallogenic model for pelitic-mafic-type VMS deposits. In Québec, the largest deposit of this type is Soucy-1 (5.4 Mt at 1.49% Cu, 1.80% Zn, 1.61 g/t Au and 13.7 g/t Ag; Wares *et al*., 1988), located about 41 km south of the village of Tasiujaq (Figure 8). This deposit is included in the set of 18 pelitic-mafic-type VMS deposits, all located in the Labrador Trough. This set of deposits corresponds to the Type 3 deposits of Clark and Wares (2004), described as "VMS-type Cu-Zn-Co-Ag-Au and Zn-Pb-Cu-Ag-Au mineralization". According to these authors, this type of mineralization is the most economically interesting in the Trough. The Soucy-1 deposit (see description by Barrett *et al*., 1988), served as the model for most of the parameters used in the processing.

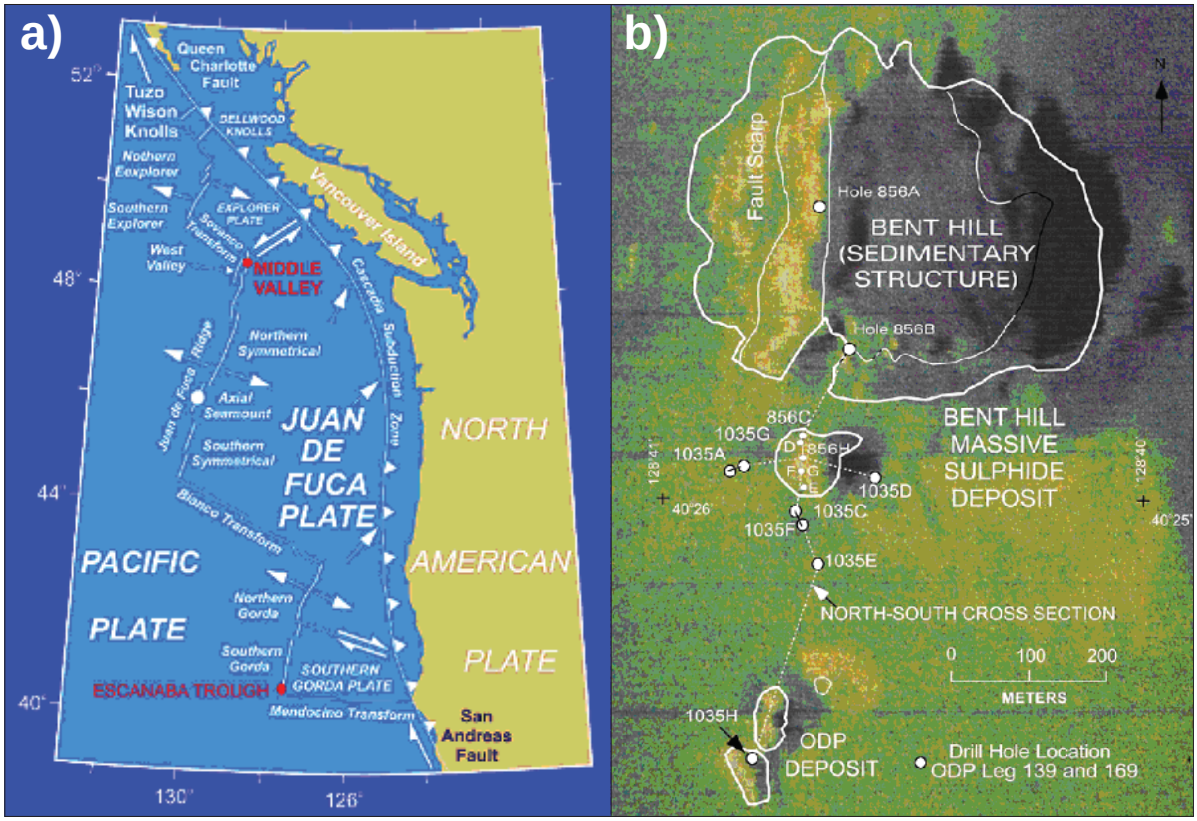


**FIGURE 6** – a) Emplacement of Middle Valley in the northern part of the Juan de Fuca ridge off the western coast of North America; b) Surface geology in the Bent Hill region showing the Bent Hill sedimentary structure with fault escarpments along the western edge, massive sulphide buttes targeted by the Bent Hill Ocean Drilling Program, and the locations of the 139 and 169 legs and their corresponding boreholes. The general geology is revealed on a SeaMARC sidescan sonar colour image (Goodfellow *et al.*, 1999). Source for both images: Geological Survey of Canada website.

**TABLE 2 –** Characteristics of pelitic-mafic-type VMS deposits

| | |
|---|---|
| **Synonymous names** | Besshi-type VMS; siliciclastic-mafic-type VMS |
| **Geometry of the mineralization** | Stratiform massive sulphides, metre-scale thickness and kilometre-scale extent. May also consist of superimposed lenses. |
| **Associated lithologies** | Terrigenous clastic sediments; lavas and basaltic to andesitic pyroclastics locally brecciated; black shale, iron oxide or silicate facies iron formations, red chert (jaspillite). |
| Age | Mainly Paleozoic and Mesozoic |
| Geological setting | Volcanic centre, extensional seafloor hydrothermal chimney, proximal downthrow fault. Presence of breccias in immediate vicinity of the deposits. |
| Tectonic setting | • Back-arc basin, continental margin rift, intracontinental rift, near-continent extensional forearc ridge. Host sequence of clastic sediments and mixed mafic volcanics.<br>• Oceanic rift or suprasubduction environments with mafic magmatism bearing thick layers of deep sedimentary rocks (argillite, siltstone, wacke) cut by mafic-ultramafic sills;<br>• According to Skulski et al. (1993), units of the second cycle of the Labrador Trough were deposited in a dextral transtensional basin developed along a continental margin. |
| Economic substances | Cu, Zn, Co, Ag, Au |
| **Indicator metals** | Cu, Zn, Pb, Co, Ag, Au, Mn. The Co/Ni ratio is greater than 1. |
| **Indicator minerals** | Pyrite, pyrrhotite, chalcopyrite, sphalerite, magnetite, valleriite, galena, bornite, tetrahedrite, cobaltite, cubanite, stannite, molybdenite, arsenopyrite, marcasite. |
| **Gangue** | Quartz, carbonate (calcite, ankerite, siderite), albite, white mica (sericite), chlorite, biotite, amphibole, tourmaline, stilpnomelane, grunerite and magnetite. At Soucy-1, stilpnomelane represents retrograde alteration of grunerite (Barrett et al., 1988). |
| **Alteration** | Chloritization, silicification, carbonatization. Albitization is noted in the sedimentary rocks. |
| Heat sources | • Sills of the Montagnais Group (Baragar, 1967; Dimroth, 1978), renamed the Montagnais Sills by Clark and Wares (2004), have been dated by three different studies: 1) 1884 ± 2 Ma (Findlay *et al.*, 1995); 2) 1874 ± 3 Ma (Machado *et al.*, 1997); and 3) 1882± 4 Ma (Wodicka et al., 2002). This 10 Ma range is contemporaneous with mafic magmatism of the second cycle of the Le Moyne Group (Hellancourt Formation). These sills constitute potential heat sources. The sediment-gabbro contact is a key feature in this model.<br>• Hydrothermal solutions may also follow downthrow faults created during back-arc basin emplacement. The heat source driving these cells is fed by the magmatic chamber below the rift. Metal enrichment of the fluids (e.g., Zn and Cu) occurs by recirculation through sedimentary units interbedded with mafic flows and sills. Downthrow faults, rarer in the internal part of the Trough, may have been re-activated as a thrust fault during closure of the orogen. |
| **Volcanic hiatus** | Fairly thick sequences of detrital sediments are characteristic of large pelitic-mafic deposits. These horizons mark a hiatus in volcanism during which sulphide deposits accumulated. |

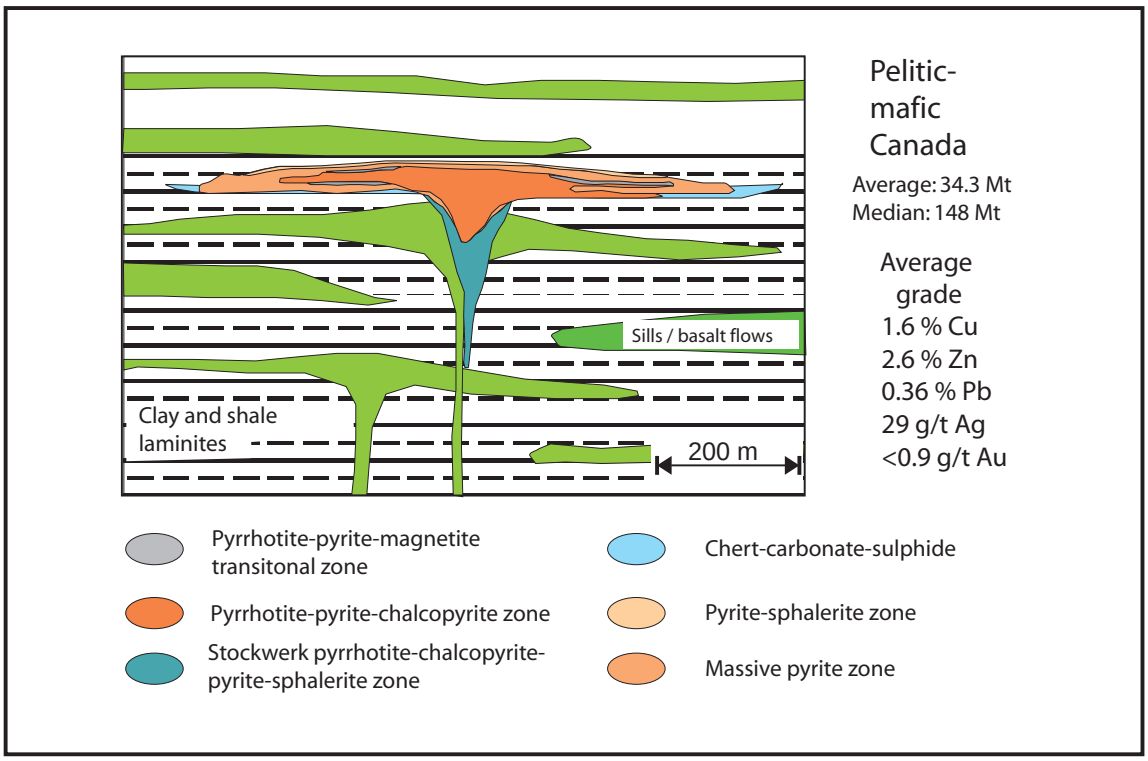


**FIGURE 7** – Schematic representation of the metallogenic model for pelitic-mafic-type volcanogenic massive sulphides (modified from Galley *et al.*, 2007).

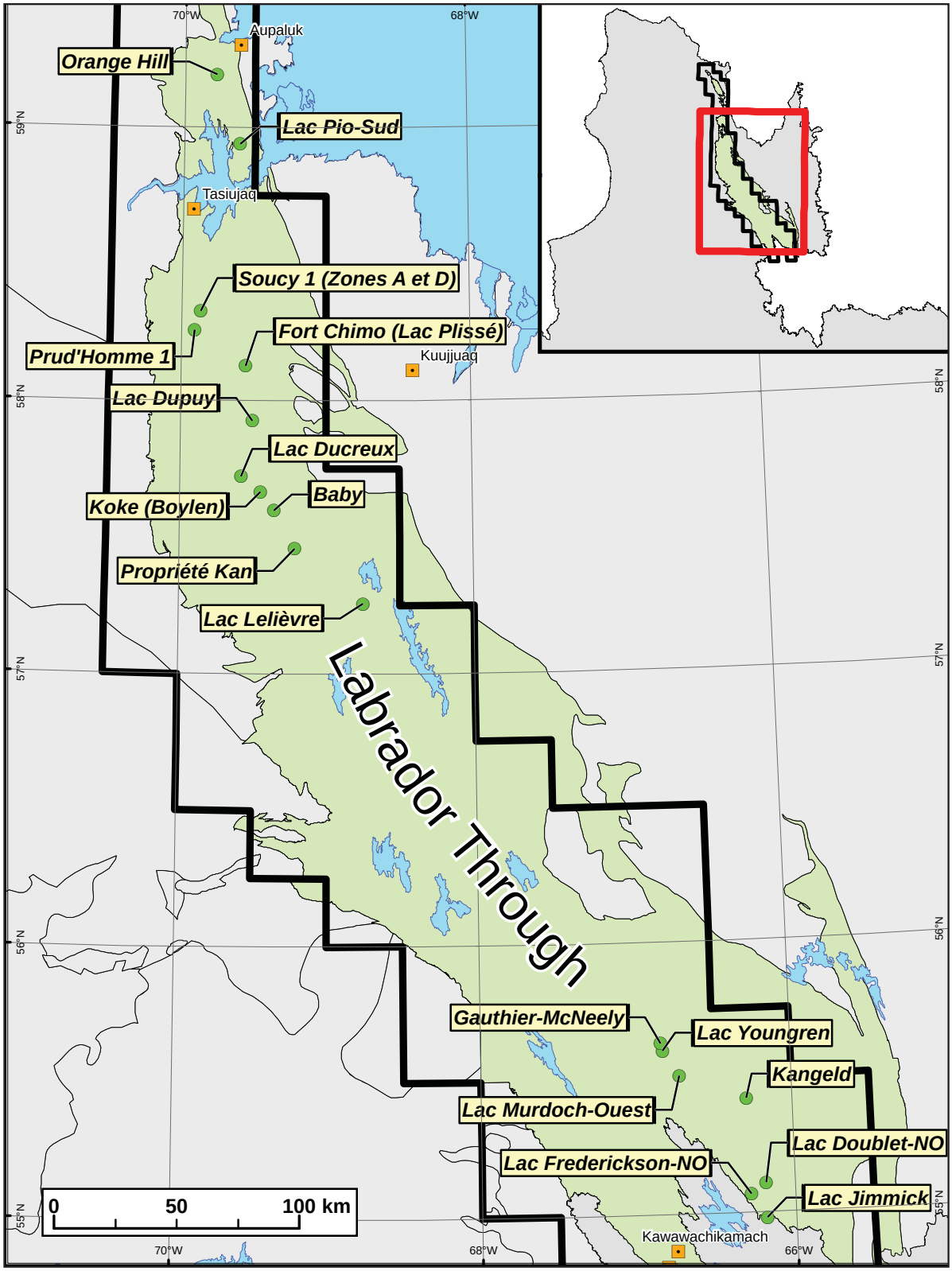


**FIGURE 8** – Location of the 18 pelitic-mafic-type volcanogenic massive sulphide deposits used in the processing and described in Appendix 1.

# METHODOLOGY FOR ASSESSING FAVOURABILITY

## Introduction

Processing methods to assess mineral potential fall in one of two main categories (Table 1): 1) empirical or data-driven methods, and 2) conceptual or knowledge-driven methods. Empirical methods are based on the analysis of spatial correlations between known mineralized occurrences and certain geological parameters. The best known empirical methods are the Weights of Evidence (WofE) method and neural network analysis. Conceptual methods are generally used in the absence of known deposits within the study area and thus rely on the knowledge and experience of a geologist to assign a relative weight to each parameter. Among these methods, fuzzy logic is by far the most commonly used, mainly due to its flexibility and simplicity.

Hybrid approaches combining the flexibility of knowledge-driven approaches with the rigour of data-driven approaches have recently been proposed (Brown *et al.,* 2003; Porwal *et al*., 2003b). One of these, known as "hybrid fuzzy logic", can be used to get around one of the main difficulties encountered with the WofE method: the underlying assumption of Bayes' theorem that all of the data used (the parameters) must be independent from one another. This condition is difficult to respect when the method is applied in a geological setting since many different categories of data are directly or indirectly derived from one of the modelling parameters (for example, contacts on a geological map interpreted from the magnetic field map). Although the approach remains valid for each parameter individually, the failure to meet the "conditional independence" clause tends to generate values that are too high, such that, when intermediate favourability maps are combined, posterior probability (resultant favourability) cannot be adequately calculated. For this reason, it was deemed more appropriate to combine parameter maps weighted with the WofE method using the fuzzy logic knowledge-driven approach (hence the term "hybrid fuzzy logic").

The selected approach is derived from the work of Porwal *et al.* (2003b) who proposed two approaches based on the concept of fuzzy logic: 1) a conceptual approach, "knowledge-driven fuzzy logic", which relies on the modeller's judgement to assign a fuzzy favourability value; and 2) a semi-empirical approach, "data-driven fuzzy logic", in which the fuzzy favourability value is established based on computations of the probability of association by the Weights of Evidence method. This second approach, already used for most metallogenic models processed at Géologie Québec (Lamothe *et al.*, 2005, Lamothe, 2008, 2009, 2011), was adopted for the present study.

## Methodology

The WofE approach has been used by Wright and Bonham-Carter (1996), Reddy *et al.* (1991) and Agterberg (1989) for VMS mineral potential assessments. The method was also used to assess the potential for orogenic gold deposits (Bonham-Carter *et al.*, 1988; Porwal and Hale, 2000; Harris *et al.*, 2001) and epithermal gold deposits (Turner, 1997; Carranza and Hale, 2000; Boleneus *et al.*, 2001), as well as for porphyry copper deposits (Carranza and Hale, 2002)[1].

This technique was developed by Spiegelhalter (1986) and applied to mineral exploration by Bonham-Carter *et al.*, (1988), Harris *et al.*, (1995), Wright (1996), Wright and Bonham-Carter (1996) and Raines (1999). According to this approach, a series of parameter maps (*evidential maps*) derived from geophysical, geochemical and geological data are combined to produce a favourability map using Bayesian statistics. The spatial association of each parameter map is calculated relative to the location of known deposits. A pair of weight factors, $W^+$ and $W^-$, is determined by the amount of overlap between known deposits and the various classes of the parameter map. If no particular association is observed between known mineral occurrences and the parameter map, then $W^+ = W^- = 0$. A positive value for $W^+$ indicates a positive association between known deposits and the parameter map. The contrast value C (where $C = [W^+] - [W^-]$) represents the degree of spatial association between the parameter map and known occurrences (Figure 9).

An overview of the deposits used to perform the weighting is presented in Appendix 1. As was done in the Abitibi VMS model update (Lamothe, 2011), each deposit was weighted as a function of its importance based on the level of exploration work. To do this, each point representing a deposit was multiplied by a factor of 1, 2 or 3 depending on whether the deposit is a showing, a worked

1 The ArcSDM module, an extension of ArcGIS provided free of charge by Natural Resources Canada, can be used to easily calculate the different variables in the Weights of Evidence method. The contrast values calculated by WofE for each parameter are provided in Appendix 2.

deposit, or a deposit with tonnage estimates. This approach enhances the predictivity of parameters that are preferentially associated with economically important deposits.

The hybrid fuzzy approach uses the WofE method to calculate a **favourability value** (Vfavor) based on the contrast value (C), according to the set of equations below (Porwal *et al.*, 2003b)[2]. Equation (1) is used if the contrast value is positive. If the contrast value is negative, then equation (2) is applied. If the contrast value is nil, then both equations will yield a favourability value of 0.5.

$$\textbf{Vfavor} = 0.5 + (C_{ij} / 2 \times C_{max}) \text{ if } 0 \leq C_{ij} \leq C_{max} \quad (1)$$

$$\textbf{Vfavor} = 0.5 - (C_{ij} / 2 \times C_{min}) \text{ if } C_{min} < C_{ij} \leq 0 \quad (2)$$

$\mathbf{C_{ij}}$ = contrast value of class *j* on parameter map *i*

$\mathbf{C_{max}}$ = maximum contrast value for all parameter maps

$\mathbf{C_{min}}$ = minimum contrast value for all parameter maps

This approach, fairly similar to the one used by Cheng and Agterberg (1999), applies the notion of **relative weighting of parameter maps** since it redistributes the favourability of each parameter according to the minimum and maximum values for all maps and classes used[3]. For the pelitic-mafic VMS model applied to the Labrador Trough, values for $C_{max}$ and $C_{min}$ are respectively 9.615 and –8.343.

The various maps generated in processing this metallogenic model are combined using fuzzy operators, some of which are equivalent to Boolean operators. Operators used in this study are GAMMA and OR. The use of the OR operator generates on output the maximum favourability value observed on combined maps. The OR operator is used to combine any parameters that represent the same geological phenomenon (for example, ISER and Sericite NORMAT indices) but are expressed differently. The GAMMA operator allows the modeller to emphasize the importance of overlap for certain favourable parameters by generating a **result higher than the maximum value of cells in combined maps**. The GAMMA operator is modulated with a gamma factor F, the value of which (generally in the range 0.80 to 0.97) is determined by the modeller and is proportional to the desired amount of emphasis.

Abuse of the GAMMA operator at various steps in the combination process may generate artificial overweighting in the final assessment, since the application of a high F factor tends to disproportionately boost favourable values. To avoid this pitfall, the different factors used for GAMMA operators were calibrated so as to obtain, for all intermediate and final combinations, a background value of about 0.5. In the present approach, this value represents the middle ground between a favourable association (positive contrast) and an unfavourable lack of association (negative contrast).

The final result of the processing is a map of favourability values for VMS mineralization in a pelitic-mafic setting. The process whereby the various parameters are integrated (the inference model**)** is illustrated in Appendix 3. Parameters are grouped into categories forming four subsets: 1) lithological control; 2) alteration; 3) mineralization; and 4) secondary environment. Grouping into subsets makes it easier to understand the process and to interpret the results.

## Level of knowledge within the study area

In addition to the known significant metallogenic potential of the Labrador Trough, this region was also chosen for its advanced level of geological exploration and the considerable volume of digital data (Table 3) generated by exploration activities.

2 Absent values (NoData) were replaced with favourability values of 0.001 to avoid propagation in the final result when the favourability maps are combined.

3 The result of this approach is that at least one of the parameter classes will have a favourability value of 1, whereas at least one other class will have a value of 0. The drawback is that it is not possible to generate an intermediate favourability map for a predictive map before going through the entire process for all the maps used in the model since the calculated favourability value depends on the minimum and maximum contrast values calculated for the entire set of maps.

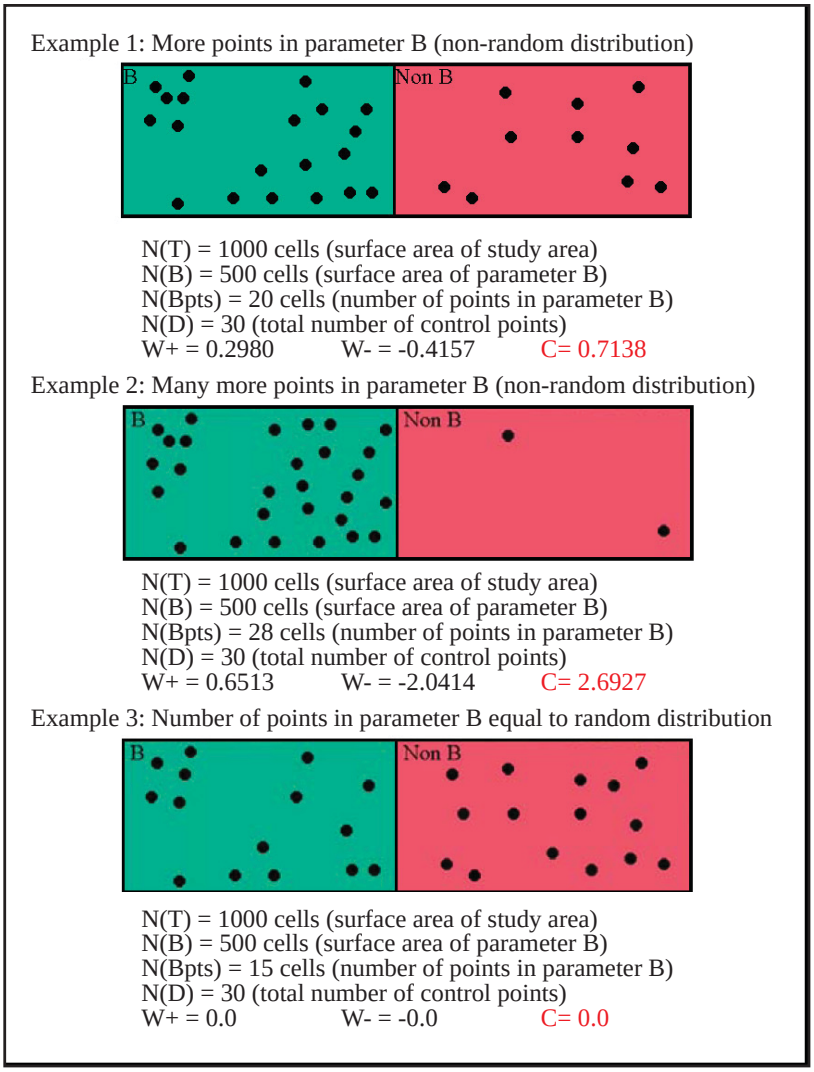


**FIGURE 9** – Examples of contrast value calculations based on the spatial association between control points and a parameter (modified from Bonham-Carter, training notes, Denver 2002).

**TABLE 3 –** Digital data available in SIGEOM for the modelling.

| Type of digital data | Number |
|---|---|
| Geological polygons | 14 297 |
| Rock analyses | 11 369 |
| Lake sediment analyses | 20 825 |
| Drill holes | 6 228 |

Figure 10 indirectly illustrates the amount of exploration work carried out in the Labrador Trough by displaying the density of available information as determined by the digital geological data compiled in SIGEOM. This provides an important context in which to consider the results of this study. A high density of information may, depending on the circumstances, explain favourable zones in some of the well-explored areas. Favourable zones in areas that have seen little or no exploration are of particular interest, suggesting that despite the paucity of geological information, some of the known features are important enough to justify an elevated potential.

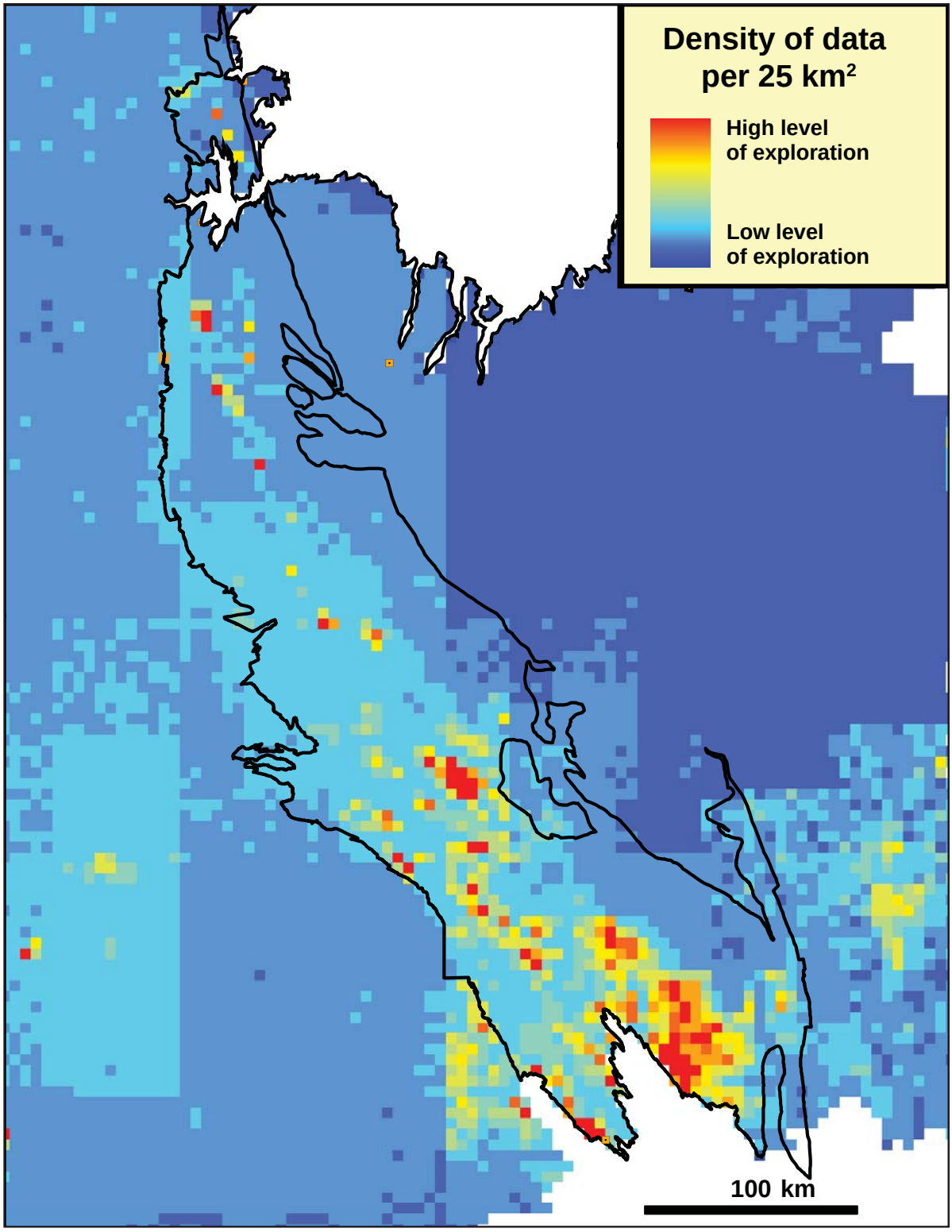


**FIGURE 10** – Extract from the geological knowledge index map of Québec of D. Lamothe (unpublished map). Density calculations were performed using all available digital geological data in SIGEOM.

# PROCESSING OF PARAMETERS

The first step consists of selecting, among all the favourable geological parameters for the presence of pelitic-mafic-type VMS mineralization, those that constitute the most effective indicators. To do this, the Weights of Evidence method (WofE; Bonham-Carter *et al.*, 1989; Harris *et al.*, 2001; Lamothe *et al.*, 2005) was used to determine the spatial association of each parameter with a set of 18 known VMS deposits in the study area (Type 3 of Clark and Wares, 2004). Only those parameters yielding a contrast value (C) above 1.5 were selected[4] (Appendix 2).

## Lithological control factor

The relevant stratigraphic units in this metallogenic model correspond to volcano-sedimentary sequences deposited in deep environments, contemporaneous with intrusions serving as heat sources and capable of activating hydrothermal cells and brecciation processes (Lydon, 1984; Franklin *et al.* 2005).

### Favourable stratigraphic unit

Only the Cycle 2 stratigraphic units (Figure 4) of Clark and Wares (2004) correspond to the above-mentioned depositional criteria. From these units, which are typical of a pelitic-mafic environment, the following lithologies were selected for use:

- terrigenous clastic sedimentary rock
- tholeiitic or andesitic tuff and breccia
- iron oxide or silicate facies iron formation
- chert, red chert or jaspillite
- basaltic volcanic rock

Following a predictivity test using the WofE method, only those units listed in Appendix 2 were retained. All units have contrast (predictivity) values above 1.8 (Appendix 2), the only exception being the undifferentiated Hellancourt Formation (code [ppro]he: Table 4 and Appendix 2), which has a low but positive calculated predictivity (0.448). This formation, essentially present in the northern part of the Labrador Trough, was kept because it appears to correlate in the south with the [ppro]he1 Hellancourt lithodeme, which is a good predictor (3.481). It should be noted that the level of detail in the map used for the present study did not allow for the representation of any of the thin (<75 m) sedimentary interbeds occurring within volcanic units horizons or between closely spaced sills of the Montagnais Suite (see following section). This explains the positive predictivity of volcanic or intrusive units in a metallogenic model in which deposits are essentially concentrated in sedimentary horizons. This is why several of the pelitic-mafic-type VMS deposits used as controls in the model (Orange Hill, Prud'Homme-1, Fort Chimo, etc.) occur in the Montagnais Suite or in the volcanic units of the Hellancourt Formation, even though their detailed descriptions indicate an association with sedimentary mudstone or iron formation assemblages.

### Proximity to an intrusion of the Montagnais Suite

The genesis of VMS deposits requires a heat source able to generate and sustain hydrothermal activity through fluid convection in volcano-sedimentary piles. The Montagnais Suite is the only magmatic heat source contemporaneous with Cycle 2 rocks[5] of the Labrador Trough[6]. These intrusions have been dated by three studies which yielded ages corresponding to the estimated age of the second cycle of Clark and Wares (2004): 1) 1884 ±2 Ma (Findlay *et al.*, 1995); 2) 1874 ±3 Ma (Machado *et al.*, 1997); and 3) 1882 ±4 Ma (Wodicka *et al.*, 2002). An indirect confirmation of the

4 The minimum threshold of 1.5 applies to the most predictive class for the parameter.

5 An age of 2169 ±4 Ma has been attributed to a sill of the Montagnais Suite (Rohon *et al.*, 1993) in the Chakonipau Formation, a basal unit belonging to Cycle 1. It is thus probable that the Montagnais Suite really comprises two distinct intrusive sequences separated by an interval of nearly 290 Ma. It is also possible that some of the sills injected into Cycle 1 rocks and used in the modelling are incompatible with the specific tectonostratigraphic setting of the tested metallogenic model.

6 The present model does not take into account the possibility of deep hydrothermal sources migrating along normal faults developed during basin subsidence, which can also generate VMS deposits. The compilation work currently underway for the Labrador Trough may define such faults, which would then be used in future version of the model.

**TABLE 4 –** List of stratigraphic units used in the processing.

| Stratigraphic unit | Stratigraphic code | Lithology |
|---|---|---|
| Aulneau Formation | [ppro]au3 | Argillite |
| Lower Baby Formation | [ppro]bb(i)1 | Mudstone, siltstone, sandstone, greywacke, phyllite |
| | [ppro]bb(i)4 | Chert |
| | [ppro]bb(i)5 | Pyritic black slate, pyritic siltstone |
| | [ppro]bb(i)9 | Slate, grey siltstone |
| | [ppro]bb(i)10 | Dolomite, calcsilicate rocks |
| Middle Baby Formation | [ppro]bb(m) | Undivided: iron formations |
| | [ppro]bb(m)1 | Iron formation: silicate facies, chert interbeds |
| | [ppro]bb(m)2 | Iron formation: carbonate and silico-carbonate facies |
| | [ppro]bb(m)3 | Iron formation: sulphide facies |
| | [ppro]bb(m)4 | Iron formation: oxide facies, chert |
| | [ppro]bb(m)5 | Chloritic schist, metabasalt |
| | [ppro]bb(m)6 | Black mudstone |
| | [ppro]bb(m)7 | Shale, slate, siltstone, sandstone |
| Upper Baby Formation | [ppro]bb(s)1 | Rhythmites: mudstone, siltstone, fine sandstone |
| | [ppro]bb(s)7 | Black graphitic mudrock, locally pyritic |
| | [ppro]bb(s)8 | Mudrock, black or dark grey slate, sandstone |
| Undifferentiated Baby Formation | [ppro]bb1 | Mudrock, phyllite, slatey schist |
| Douay Formation | [ppro]da4 | Basalt |
| | [ppro]da5 | Shale, slate, siltstone, pelitic schist |
| Hellancourt Formation | [ppro]he | Basalt, some tuff and breccia |
| | [ppro]he1 | Pillowed basalt |
| | [ppro]he2 | Massive basalt |
| | [ppro]he3 | Mudrock, locally pyritic |
| | [ppro]he4 | Mafic pyroclastic rocks |
| | [ppro]he5 | Plagioclase-phyric basalt |
| Menihek Formation | [ppro]me1 | Mudstone, siltstone, phyllite, slatey schist |
| | [ppro]me9 | Sulphide facies iron formation |
| Willbob Formation | [ppro]wl | Basalt, breccias, tuff, fine sediments and gabbro |
| | [ppro]wl4 | Mudrock, tuffaceous mudrock and pyritic mudrock |
| | [ppro]wl5 | Sulphide iron formation |

role played by the Montagnais Suite is the fact that all known VMS deposits in the Trough, with the exception of the Koke deposit, are found less than 1 km from an intrusion belonging to this unit. However, the low predictivity of this parameter (22$^{nd}$ rank, Appendix 2) is due to its considerable coverage in the study area (about 16% of the surface area), which greatly increases the probability that a deposit occurs near these rocks by chance.

**Presence of breccias**

The deposition of sulphides on or below the seafloor sometimes seals the hydrothermal vent and causes explosive hydrothermal or hydrovolcanic processes (Lydon, 1984; Franklin *et al.* 2005). This leads to brecciation of the sulphide deposits and adjacent rocks, thereby favouring the emplacement of stockwork systems. A stockwork is a significant indicator of potential proximity to a VMS deposit.

Numerous examples of brecciated volcanic or sedimentary rocks were extracted from the textural drill hole descriptions in SIGEOM. These occurrences are good indicators (9$^{th}$ rank, Appendix 2) of proximal VMS mineralization.

## Hydrothermal alteration factor

The deposition of massive sulphides near volcanic vents in a submarine environment is related to fluid circulation in large hydrothermal cells responsible for the widespread leaching of metals and localized precipitation on the seafloor (Galley, 1993; Franklin, 1995). The actions of these cells are accompanied by alteration processes semi-concordant to the country rocks (Figure 5).

Based on the available data for the Labrador Trough region, alteration indicators can be grouped into two main subsets: 1) chemical alteration indicators determined by various calculated petrochemical indices; and 2) minerals indicative of alteration processes associated with VMS deposits.

### Chemical alteration indicators

Two alteration indices among nine calculated by CONSOREM's LithoModeleur software are considered to be good indicators of chemical alteration. The indices were calculated using a subset of 443 volcanic samples, predominantly basaltic.

#### *Proximity to an anomalous Hashimoto index*

The Hashimoto index (Ishikawa *et al*., 1976) is represented by the equation: $(FeO_t+MgO+K_2O+4)/(MgO+K_2O+CaO+Na_2O)$. It applies to rocks ranging in composition from basaltic to rhyodacitic. Based on the LithoModeleur classification, a total of 144 samples with low or high Hashimoto index values were selected and their predictivity tested with WofE. Predictivity is high up to a distance of 400 m and remains favourable up to 2,200 m, ranking it 19$^{th}$ (Appendix 2).

#### *Proximity to an anomalous Sericite index*

LithoModeleur software uses a variant of the Sericite index (Saeki and Date, 1980) with the equation $K_2O+1$ instead of $0.5(K_2O+Na_2O)$. Only the 63 samples with elevated alteration values were tested using the WofE method. This parameter is very favourable up to a distance of 400 m and ranks 16$^{th}$ in terms of predictivity (Appendix 2).

#### *Proximity to an anomalous NORMAT alteration index*

Evidence of hydrothermal activity may manifest as anomalous concentrations of normative minerals in igneous rock analyses. The normative mineral indices ISER and IFRAIS[7], calculated using NORMAT software, were used to quantify alteration regardless of the original composition of the rock (Piché and Jébrak, 2004). These computations were conducted on a database of 4,789 major element analyses for intrusive and extrusive rocks.

#### *Proximity to an anomalous ISER index*

A quantile-quantile plot was constructed with all 548 analyses yielding a non-nil ISER index. The anomalous threshold thus determined corresponds to ISER values equal to or greater than 6.5% (Figure 11). Distance buffers at 200-m intervals were defined around the resulting 68 samples and contrast values were calculated with WofE (Appendix 2). This parameter is effective up to a distance of 600 m and ranks 20$^{th}$ in terms of predictivity.

#### *Proximity to an anomalous IFRAIS index*

The procedure described above for determining an anomalous threshold for the ISER index was also applied to 4,789 samples with calculated IFRAIS indices. Those with IFRAIS values below 77% were retained (Figure 11). The 3,545 selected samples were buffered using 200-m intervals and contrast values were calculated and optimized with WofE (Appendix 2). This parameter is effective up to a distance of 400 m and ranks 18$^{th}$ in terms of predictivity.

7 The NORMAT ICHLO index was also tested but did not prove to be a good indicator.

**Alteration mineral indicators**

This group of parameters models the predictivity of various mineralogical indicators of alteration processes affecting host rocks to mineralization. The three parameters below were mainly defined using the work of Barret *et al.* (1988) on the Soucy-1 deposit. Each parameter was processed based on local occurrences (documented in outcrop descriptions (*géofiches*), compilation outcrop descriptions (*compifiches*) and drill hole descriptions) of one or more minerals specifically associated with each indicator.

***Proximity to carbonate alteration***

*Géofiches* and drill hole descriptions mentioning volcano-sedimentary rocks affected by carbonate alteration were extracted by query (111 occurrences). Distance buffers at 200-m intervals were created and optimized into three predictive distance classes with WofE (Appendix 2). This parameter is effective up to 2,800 m and ranks 13$^{th}$ in terms of predictivity.

***Proximity to iron alteration***

Descriptions of magnetite, stilpnomelane, grunerite, chlorite or magnetite alteration were extracted from *géofiches*, compilation outcrop descriptions and drill hole descriptions mentioning volcano-sedimentary rocks. The 353 point occurrences thus obtained were buffered at 200-m intervals and contrast values were calculated and optimized into three predictive distance classes with WofE (Appendix 2). This parameter is effective to a distance of 2,800 m and ranks 6$^{th}$ in terms of predictivity.

***Presence of graphite***

Graphitic or carbonaceous material is often mentioned in the majority of large pelitic-mafic-type VMS deposits. This type of material is a component of country rocks at the Windy Craggy mega-deposit, as well as most other deposits used in the present model. Graphite is reported in 909 drill hole or compilation outcrop files with volcano-sedimentary rock associations. The parameter is predictive to a distance of 400 m and ranks 11$^{th}$ in terms of predictivity.

**Sulphide or oxide mineralization**

This subset of the model groups local observations of sulphide or oxide mineralization derived from *géofiches*, compilation outcrop descriptions and drill hole descriptions in the study area. Targeted minerals include pyrite, pyrrhotite, chalcopyrite, sphalerite and magnetite. All of these minerals have been recognized in pelitic-mafic-type VMS deposits, sometimes on their own but more commonly in polymineralic assemblages (Franklin *et al*., 2005). For each indicator described below, point occurrences from *géofiches*, compilation outcrop descriptions and drill hole descriptions in volcano-sedimentary rocks were buffered at 200-m intervals and contrast values were calculated and optimized with WofE (Appendix 2).

***Proximity to pyrite mineralization***

Pyrite is one of the most common sulphide phases and was reported in 1,111 different locations in the Labrador Trough. It is a good proximity indicator and remains predictive to a distance of 2,000 m. It ranks 12$^{th}$ in terms of predictivity.

***Proximity to pyrrhotite mineralization***

Similar to pyrite, the presence of pyrrhotite is commonly reported in the study area (1,045 observations). It is also a very good proximity indicator and is reliable to a distance of 2,400 metres. This parameter ranks 7$^{th}$ in terms of predictivity.

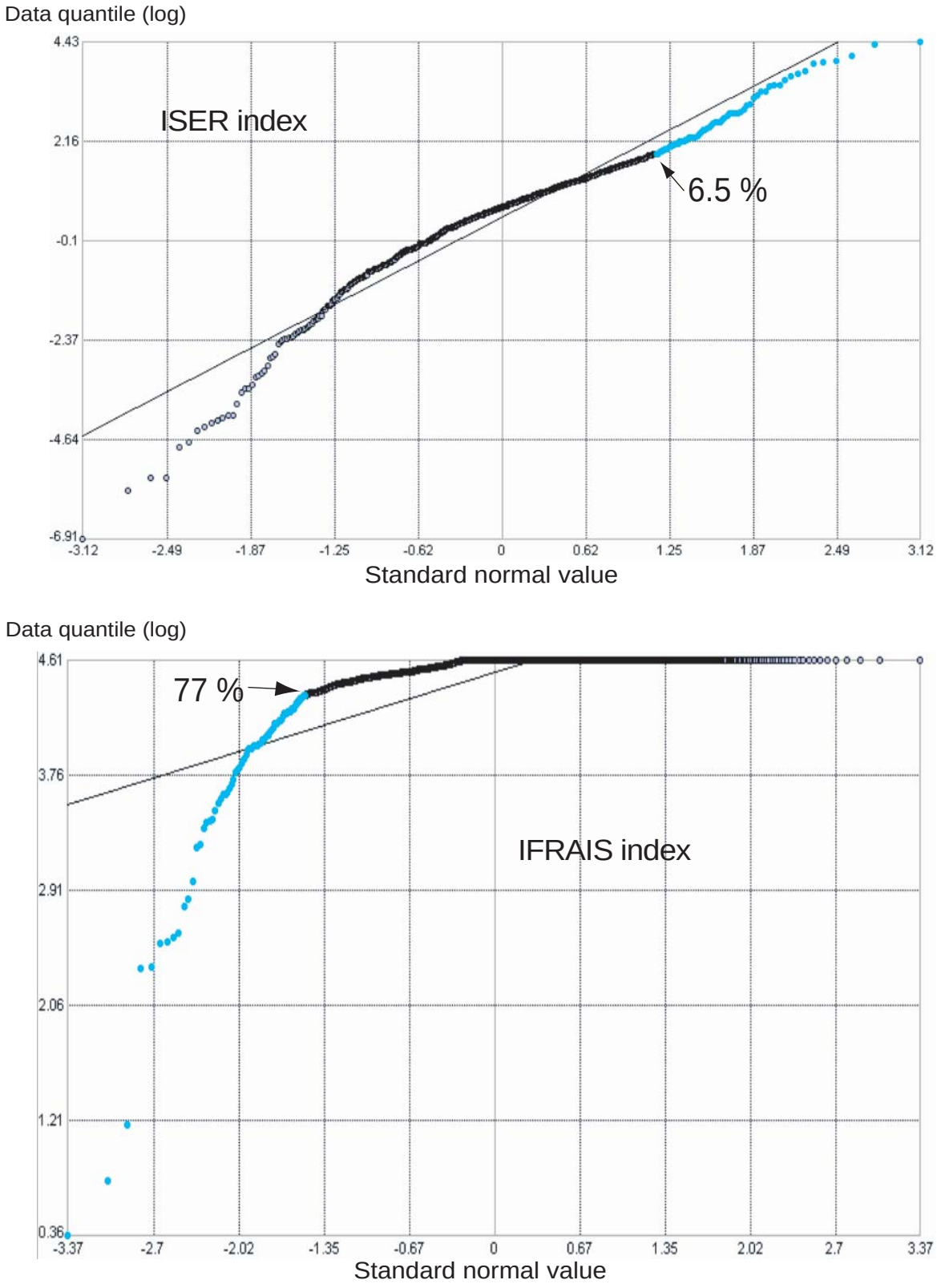


**FIGURE 11** – Quantile-quantile plots showing the ISER and IFRAIS normative indices calculated using NORMAT software (Piché and Jébrak, 2004). Anomalous thresholds are above 6.5% for ISER and below 77% for 77% for IFRAIS.

***Proximity to chalcopyrite mineralization***

A total of 678 chalcopyrite observations are documented for the Labrador Trough. This parameter is a very proximal indicator and remains predictive to a distance of 2,000 metres. It ranks 5th in terms of its predictivity (Appendix 2). Its proximal association and good predictivity make it a very effective parameter for this ore deposit model.

***Proximity to sphalerite mineralization***

Only 71 observations of sphalerite are reported for all the drill holes in the study area. This parameter is an excellent indicator to a distance of 800 m. The low number of observations, however, makes this parameter's effective distance somewhat doubtful.

***Proximity to magnetite mineralization***

This parameter is based on all observations of magnetite as an accessory mineral, not as an alteration mineral. The large number of occurrences (1,501 cases) confirms it is a very common mineral. It is a valid predictor up to 1,000 m and ranks 21st.

**Indicator metal analyses**

This subset of parameters groups together indicator metals derived from the available lithochemical analyses in the study area. The analyses were obtained from geological surveys, drill holes or the results of assessment work. Seven metals – copper, zinc, lead, cobalt, silver, gold and manganese – have proven to be excellent proximity predictors for VMS deposits and are commonly associated with pelitic-mafic-type mineralization (Franklin *et al*., 2005; Galley *et al*., 2007). They are all present in strong concentrations at the Soucy-1 deposit (Barret *et al.*, 1988). All results used in this section were filtered to eliminate samples with values of Ni > 200 ppm, U > 1 ppm or Th > 2 ppm in order to eliminate metal associations that are inappropriate for the present model and are indicative of other well-known deposit types in the Labrador Trough (magmatic Cu-Ni, vein-type U ± Cu ± Au, etc.). Only data from volcano-sedimentary rocks were used. All thresholds used to extract the results were established based on the work by Barret *et al*. (1998) on the principal lithologies of the Soucy-1 deposit.

***Proximity to a copper anomaly***

The threshold for Cu was established at 500 ppm, corresponding to 214 occurrences when taking into account the constraints specified above. Anomalous samples were buffered at 200-m intervals and contrast values were calculated with WofE. This step allowed us to determine that the parameter is predictive to a distance of 2,500 m (Appendix 2).

***Proximity to a zinc anomaly***

The anomalous threshold for zinc was established at 500 ppm, corresponding to 142 cases, most of which occur in the central and southern parts of the Trough. This parameter remains a good predictor up to 1,000 m and an acceptable predictor up to 2,800 m (Appendix 2). Its excellent proximity predictivity (<400 m) ranks it 3rd among all parameters.

***Proximity to a lead anomaly***

In the SIGEOM database, there are 92 analyses with lead values greater than 100 ppm, most of which are located in the central part of the Trough. This parameter is highly predictive (ranking 1st in the list) at distances less than 400 m and remains effective to 1,000 m (Appendix 2). Its excellent predictivity is due to the small number (92) of analyses exceeding the selected threshold and their proximity to most of the deposits considered in the model.

***Proximity to a cobalt anomaly***

With a threshold of 100 ppm and an effective distance of 400 m, cobalt ranks 18th in terms of predictivity. The great majority of these cases occur in the central part of the Trough.

***Proximity to a silver anomaly***

Using a threshold of 2 ppm for silver, 159 occurrences were identified throughout the Trough, with a slightly higher concentration in the central part. This parameter remains predictive to a distance of 2,800 m and ranks 15th.

***Proximity to a gold anomaly***

All analyses with more than 100 ppb gold were retained, for a total of 146 occurrences spread fairly evenly throughout the central and southern parts of the Trough. This parameter is one of the most effective, ranking 2nd and maintaining excellent predictivity up to a distance of 800 m.

***Proximity to a manganese anomaly***

The lithologies hosting mineralization at the Soucy-1 deposit contain significant manganese anomalies (Barret *et al*., 1998). Using a threshold of 1,000 ppm, 1,095 occurrences were retained for the predictivity calculation. The parameter has good predictivity up to a distance of 400 m and ranks 14th in the list.

## Secondary environment indicators

This section is the result of numerous attempts to define a set of samples constituting the best possible secondary environment indicators for VMS deposits. Several techniques, namely spatial regression (Trépanier, 2007; Lamothe, 2010), targeting by the U-statistics method (Cheng *et al.*, 1996; Cheng, 1999) and principal component analysis were all tested and rejected due to their low predictivity when tested with WofE. The method that generated the best predictivity results is one that uses a threshold of two standard deviations (2σ) above the mean of converted natural logarithm values. Among the seven elements used for rocks (preceding section), only three (Cu, Zn and Co) in the Labrador Trough lake sediment database have already been levelled by the different analytical methods used (Lamothe, 2010).

The contrast value of lake sediments is almost always low compared to other parameters because the sampled lakes are generally located several hundreds to thousands of metres from the deposits used to assess predictivity. Despite their low rankings (23th, 24th and 25th, Appendix 2), lake sediments nonetheless represent good indicators as they constitute objective data dispersed throughout the study area.

More than 5,600 stream sediment samples are available for the Labrador Trough, however these samples were not incorporated into the processing. The coverage of the study area is not homogenous and there are no stream sediment samples within several kilometres of most of the VMS deposits. For these reasons, it was not possible to determine a suitable approach to calculate this parameter's predictivity.

**Proximity to a copper anomaly**

The 2σ threshold yielded 217 samples with copper grades above 254 ppm. These samples are spread throughout the study area, although nearly half are concentrated in the Doublet Group at the southern end of the Trough. The parameter has acceptable predictivity up to a distance of 3,500 m and ranks last in the list (25th, Appendix 2).

**Proximity to a zinc anomaly**

The parameter comprises 391 anomalous samples with zinc values above 473 ppm. They are mainly concentrated in the Ferriman Group in the Schefferville and Lake Cambrien areas (Clark

and Wares, 2004), in the southwest end of the Trough. The contrast value is effective up to 1,000 m and remains acceptable up to 4,000 m.

#### Proximity to a cobalt anomaly

The 2σ threshold allowed 223 samples to be extracted with cobalt values above 60.7 ppm. These samples are distributed fairly evenly from north to south in the Trough, with a slightly higher concentration in the Doublet Group. It is the best proximity indicator of the three secondary environment parameters and it remains effective up to a distance of 2,000 m.

## POTENTIAL FOR PELITIC-MAFIC-TYPE VMS MINERALIZATION IN THE LABRADOR TROUGH

This section focuses on the step to combine parameter maps generated by the preceding section into intermediate subsets. This step allows the modeller to intervene in the processing; up to this point, the influence of each parameter had only been empirically measured based on the spatial associations between geological data. As mentioned earlier, for the parameter maps to be combined using a fuzzy logic approach, contrast values calculated by WofE must have already been converted to fuzzy values spread evenly between the highest value and lowest value for the entire set of parameters. This transformation is performed for all parameters in the Modelbuilder model after the empirical calculation using WofE, and a fuzzy bitmap image is then created for each parameter using the converted values.

Two fuzzy operators, GAMMA and OR[8], were used to create intermediate subsets (Appendix 3). The various factors for the fuzzy GAMMA operators (in parentheses on the figure in Appendix 3) were calibrated using, as a primary constraint, the requirement of obtaining a background value of 0.5 for all subset maps as well as the final map[9].

### Map of favourability associated with lithological control

Figure 12a displays various parts of the study area where lithological control has the most influence in the selected ore deposit model. The combination of the three parameter maps associated with lithological control was performed with a GAMMA operator to which a factor of 0.918 was applied. The maximum value on this map is 0.908.

### Map of favourability associated with alteration

The alteration subset map (Figure 12b) is generated by combining two intermediate subsets: chemical alteration and alteration minerals.

#### Map of favourability associated with chemical alteration

The chemical alteration map is a two-step process. The Sericite index map is first combined with the ISER normative mineral alteration index map using an OR operator (both these indices measure the same type of potassic alteration). The product of this operation is then combined with the maps for the Hashimoto and IFRAIS alteration indices. This second operation is performed using a GAMMA operator with a factor of 0.9615. The maximum value on the chemical alteration map is 0.962.

#### Map of favourability associated with alteration minerals

The map of favourability associated with alteration minerals is obtained by combining the three parameters of this category (Appendix 3) using a GAMMA operator to which a factor of 0.9615 was applied. The maximum value on this map is 0.983.

8 See section 2.2 for an explanation on the use of these operators.
9 This constraint is based on the assumption that poorly explored parts of the study area (see Figure 10) are considered neither favourable nor unfavourable for the type of mineralization targeted in the present model.

### Creation of the map of favourability associated with alteration

The map of favourability associated with alteration (Figure 12b) documents zones of the study area where hydrothermal activity played a significant role in the selected ore deposit model. It was created by combining the chemical alteration and alteration mineral maps using an OR operator (both maps represent similar evidence of alteration).

The majority of the most favorable areas coincide with the locations of pelitic-mafic-type VMS deposits. Some notable exceptions: two zones between 50 and 80 km NW of Kangirsuk and one zone 55 km NW of Schefferville; neither of these zones correspond to any known VMS deposits.

## Map of favourability associated with mineralization

The image for the mineralization subset (Figure 13a) is generated by combining the maps for two intermediate subsets: sulphides/oxides and indicator metals.

### Map of favourability associated with sulphides or oxides

The map of favourability associated with sulphides or oxides is the result of combining five parameters in this category (Appendix 3) using a GAMMA operator with a factor of 0.9727. Except for chalcopyrite, sphalerite and pyrrhotite, which rank in the top third of the ranking for parameter predictivity, all other minerals are less effective indicators, plotting in the middle or lower third.

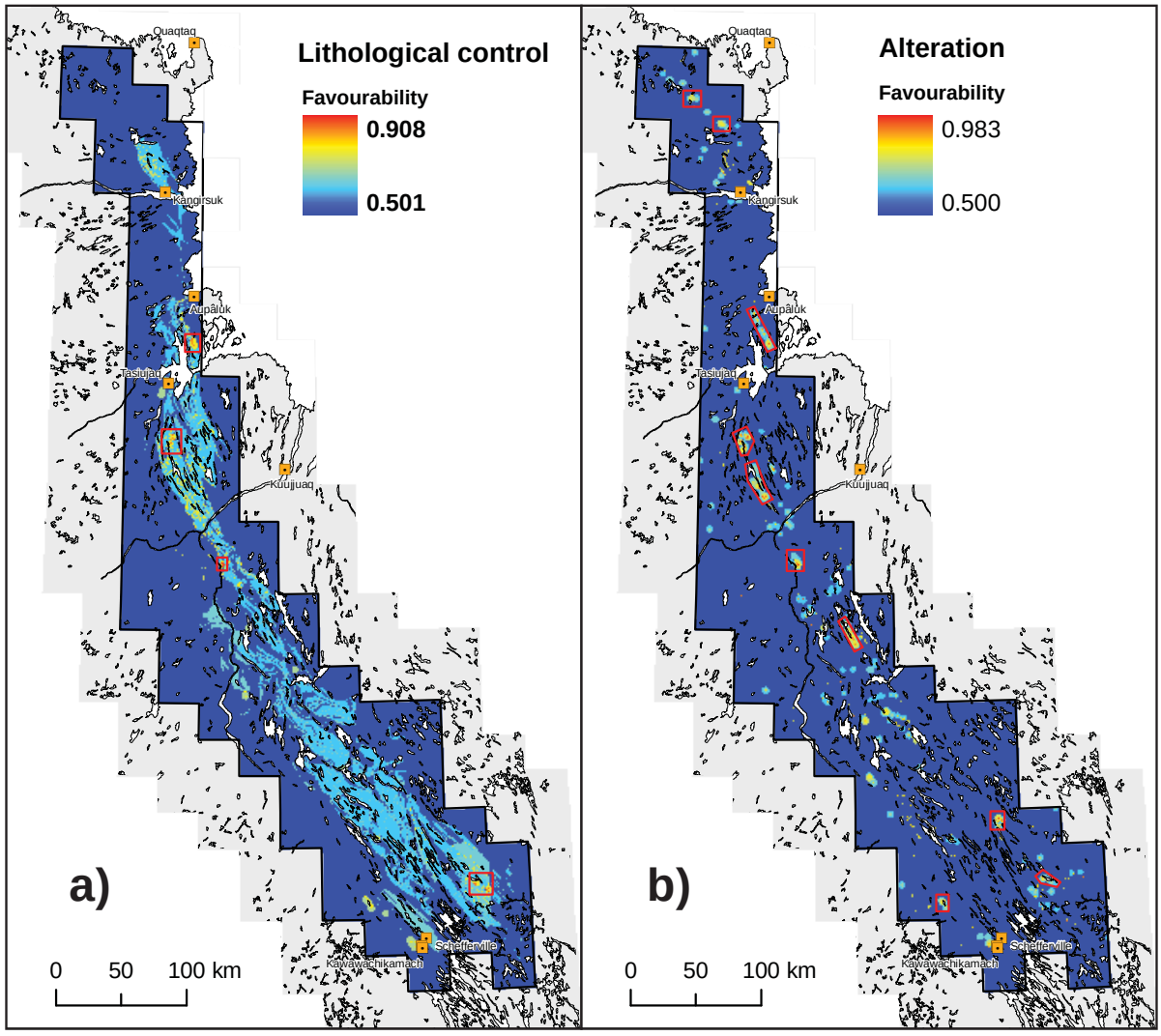


**FIGURE 12** – Favourability maps: **a**) lithological control; **b**) alteration (chemical and mineralogical). Red polygons indicate the most favourable areas.

### Map of favourability associated with indicator metals

This favourability map is generated by combining the seven indicator metals specified in the section "Indicator metal analyses". The maps were combined with a GAMMA operator to which a factor of 0.9455 was applied. The maximum value of the resultant map is 0.947. The combination emphasizes areas where more than four metals overlap.

### Map of favourability associated with mineralization

The map of favourability associated with mineralization (Figure 13a) was generated with an OR operator since the two combined maps represent data of a common nature (sulphides vs metal content). The resultant image targets a dozen areas mostly concentrated at the base of the Retty and Gérido zones (Clark and Wares, 2004).

## Map of favourability associated with the secondary environment

The map of favourability associated with the secondary environment (Figure 13b) was obtained by combining, using a GAMMA operator with a factor of 0.819, the three lake sediment maps for copper, zinc and cobalt presented in the section "Secondary environment indicators". The majority of the most favourable zones are concentrated in the Gérido and Retty zones, the latter of which contains an extensive anomalous zone more than 60 km long by 25 km wide.

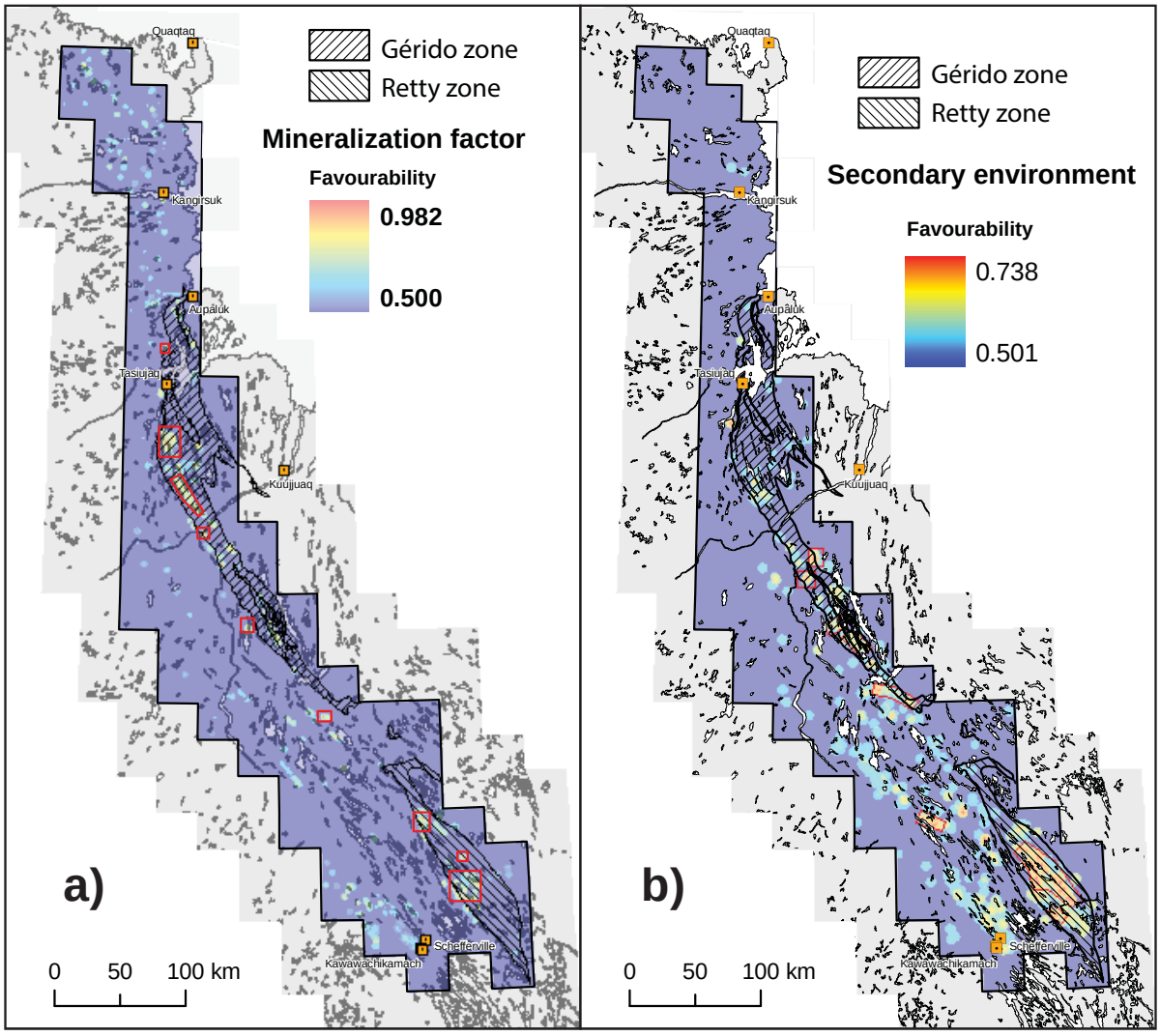


**FIGURE 13** – Favourability maps: **a**) of the mineralization factor (sulphides or oxides and indicator metals); **b**) of the secondary environment. Red polygons indicate the most favourable areas.

## Map of favourability associated with geological factors

The map of favourability associated with geological factors (Figure 14a) represents the combined contribution of all geological proximity indicators associated with the presence of pelitic-mafic-type VMS mineralization. This map was obtained by combining the maps of lithological control, alteration and mineralization. A GAMMA operator with a factor of 0.713 was used for this purpose.

## Favourability map for pelitic-mafic-type VMS mineralization

Figure 14b presents the favourability map for mineralization obtained by combining, using an OR operator, the favourability map for geological proximity factors with that of the secondary environment. This map represents the end result of a combination process involving the integration of maps from the four broad categories in the model and is the final map of the potential of the Labrador Trough for pelitic-mafic-type VMS mineralization. The maximum value of this map is 0.957.

## Determination of high-favourability zones

It is now possible to define, using the final favourability (mineral potential) map, high-favourability zones (HFZs) associated with pelitic-mafic-type VMS mineralization that can be used to focus mineral exploration efforts.

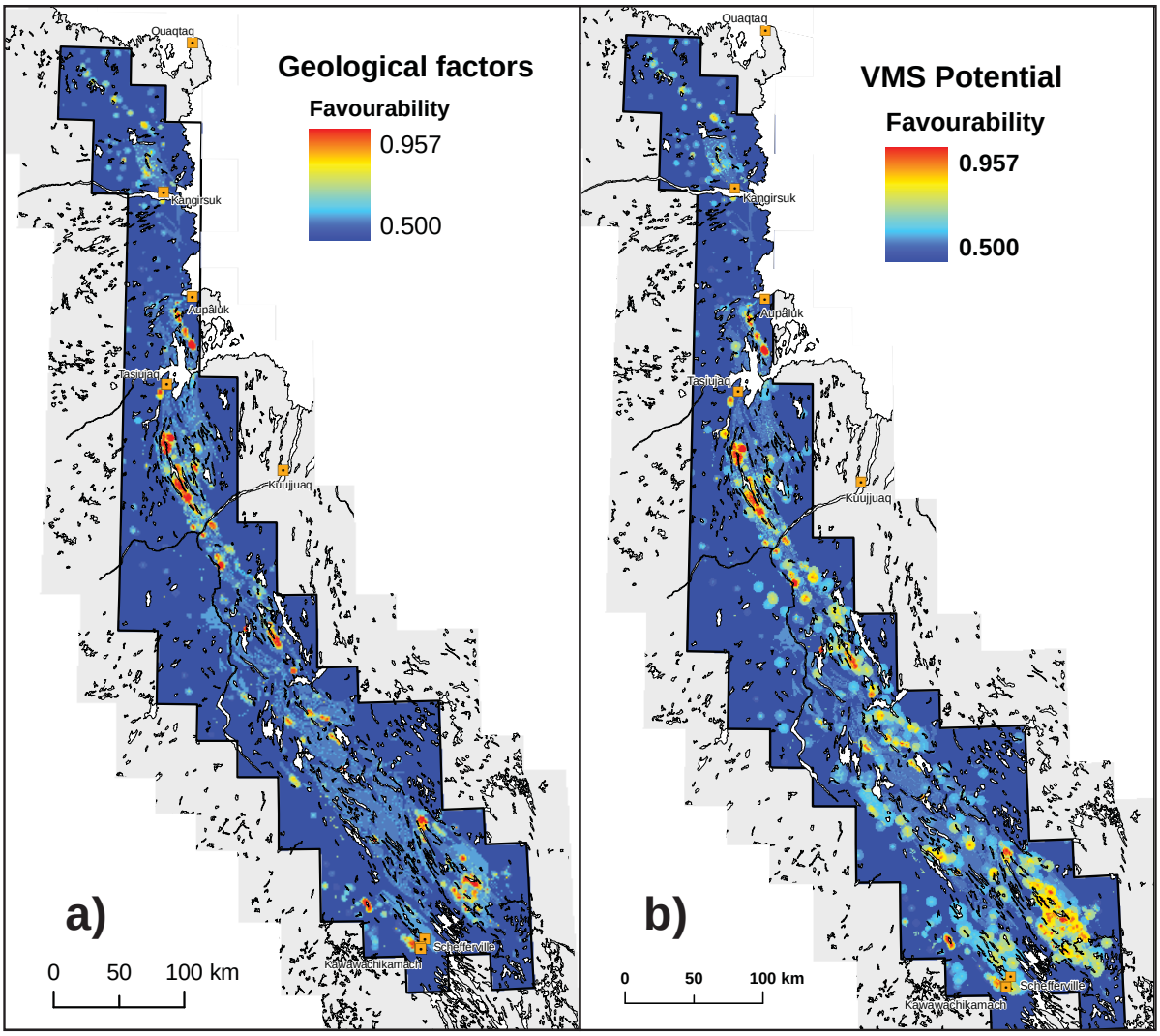


**FIGURE 14** – Favourability maps: **a**) of proximal geological factors; and **b**) of pelitic-mafic-type VMS mineralization, obtained by combining the favourability map of proximal geological factors with the favourability map of the secondary environment.

To define a high-favourability zone, a minimum favourability threshold must be established beyond which the favourability of a zone acquires significant predictivity for the presence of the targeted mineralization type. To define this threshold, the final favourability values for 18 VMS deposits in the Labrador Trough were plotted on a normal probability diagram (Figure 15), which shows two distinct normal populations. The most important (red dots) includes 8 (44%) of the 18 documented VMS deposits in the region and lies above the standard normal value threshold of 0.729 (Figure 15). All 8 deposits are worked or have tonnage estimates; the level of geological knowledge defining these deposits is sufficient to adequately target them using the present model. Conversely, the 6 showings used in the model lie below the minimum favourability threshold, as do 3 worked deposits (Lac Youngren, Gauthier-McNeely and Lac Lelièvre) and 1 deposit with tonnage estimates (Lac Jimmick). The model cannot effectively target this second population because the available data are insufficient or contradictory.

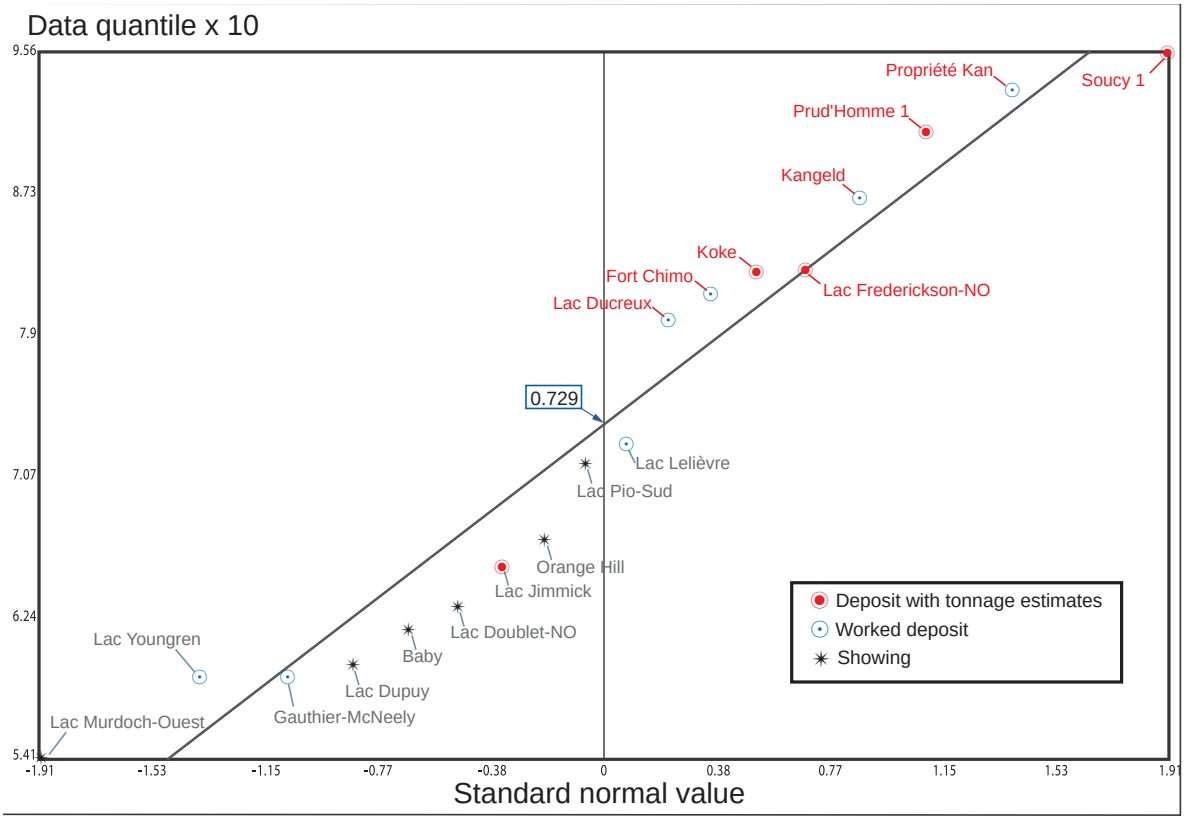


**FIGURE 15** – Determination of the minimum high-favourability threshold using a normal probability plot. Values observed on the y-axis correspond to the favourability value measured on the final favourability map for each of the 18 VMS deposits. This type of diagram is used to distinguish different populations within a set. 44% of all VMS deposits in the Labrador Trough have favourability values above 0.729 (in red) and form a homogeneous population that meets the model criteria, with measured favourability values following a Gaussian distribution. The 10 deposits in grey fall below the high-favourability threshold and do not respond well to the model.

Using the minimum threshold value, it is possible to define, based on the final favourability map, a set of cells with values equal to or greater than 0.729 and to convert these groups of cells into polygons. These polygons were combined to create 79 high-favourability zones (Figure 16). The table of attributes for each zone incorporates the maximum values for five subsets (lithological controls, alteration, mineralization, indicator metal content and secondary environment) as well as the maximum value for VMS potential for the area covered by the zone.

## Assessing the effectiveness of the map

As shown in Figure 15, all known VMS-mineralized bodies plotting above the high-favourability threshold are deposits with tonnage estimates or worked deposits. The model is thus quite effective

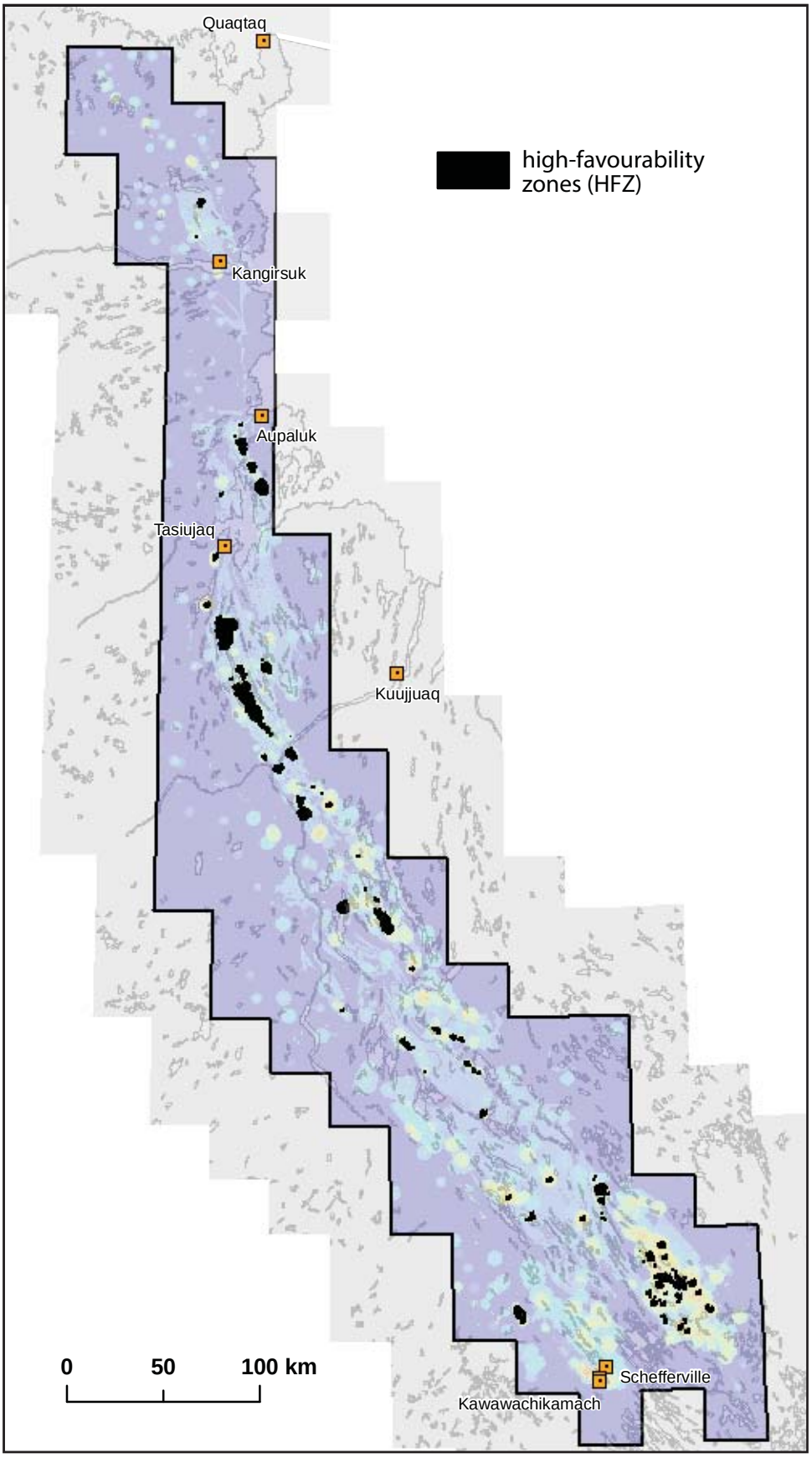


**FIGURE 16** – Location of the 79 high-favourability zones (in black) for pelitic-mafic-type VMS mineralization in the Labrador Trough. For more details, see the map accompanying the report.

for targeting this deposit type; only one of the five deposits with tonnage estimates and three of the seven worked deposits plot below the minimum threshold. None of the showings are targeted by the HFZs created during the preceding step.

The diagram in Figure 17 illustrates the predictivity of the favourability map based on the 18 VMS deposits used in this study. It indicates the cumulative percentage of the targeted deposits (on the y-axis) as a function of the surface (cumulative percentage) occupied by map cells sorted in decreasing order of favourability value (on the x-axis). The close-up of the left part of the diagram shows that 71% of the VMS deposits are predicted by 5% of the surface area with the highest favourability rating. This map is less effective than those for previous mineral potential studies (Lamothe *et al.*, 2005; Lamothe et Harris, 2006; Lamothe, 2008; Lamothe, 2009; Lamothe, 2011), which obtained proportions between 89 and 100% of the deposits with the same 5% of the highest-favourability surface area. This difference is most likely due to the decision to use deposits classified as showings to calculate predictivity. The superior effectiveness of certain deposit types (particularly mines and deposits with tonnage estimates) to define the mineral favourability of an area has been clearly demonstrated by Lamothe and Harris (2006) and by Harris and Sanborn-Barrie (2006). Mines, deposits with tonnage estimates, worked deposits, and showings are generally characterized by a respectively decreasing amount of spatial data, namely in terms of drill hole data and rock analyses. In particular, the greater volume of data associated with mines and deposits with tonnage estimates contributes to a robust definition of their geological attributes and therefore their eventual association with a parameter. Conversely, showings are commonly studied to a lesser extent and their immediate surroundings are generally poorly characterized, and this lower level of knowledge negatively impacts a certain number of parameters (lack of drill hole observations, limited sampling, deficient classification). Although useful – and even necessary in this case – the presence of these mineralized bodies in the modelling contributes to diluting the predictivity of most parameters.

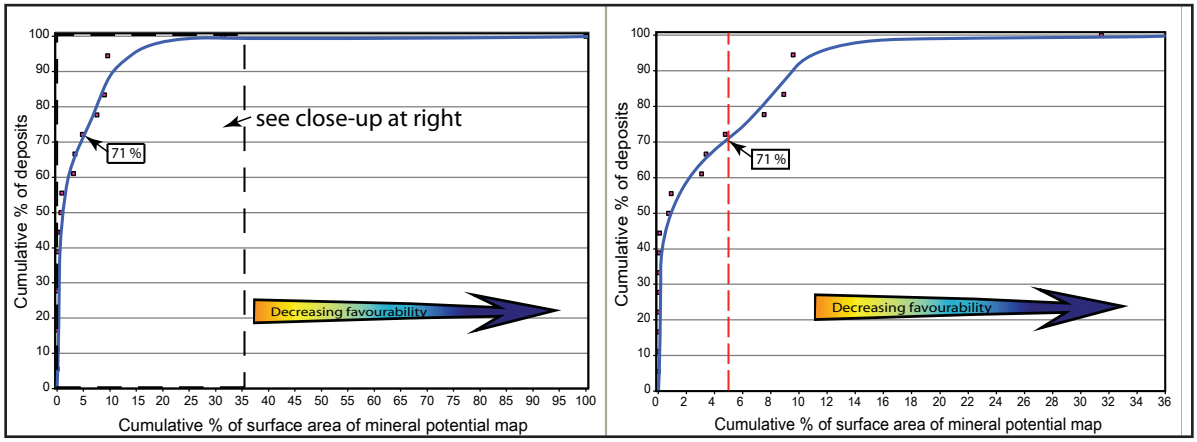


**FIGURE 17** – Diagram illustrating the predictivity of the final favourability map. About 71% of the 18 VMS-type deposits used for processing are located in the most favourable cells corresponding to 5% of the surface area on the map.

## CONCLUSIONS

The modelled integration of 25 geological parameters using hybrid fuzzy logic resulted in the production of a mineral potential map that predicts the probability of finding a mafic-pelitic-type volcanogenic massive sulphide deposit in the Labrador Trough.

Figure 18 presents a combination of the HFZ distribution map (Figure 16) and the knowledge map (Figure 10). Two conclusions can be drawn from this representation: 1) the higher level of knowledge in the southern half of the Trough and south of Tasiujaq may explain the higher concentrations of HFZs in these areas (Soucy-1 and Prud'homme-1 deposits); and 2) a number of HFZs (red polygons on Figure 18) occur in areas with low levels of exploration and no known VMS deposits in their vicinities. These areas are theoretically more favourable for the discovery of new deposits.

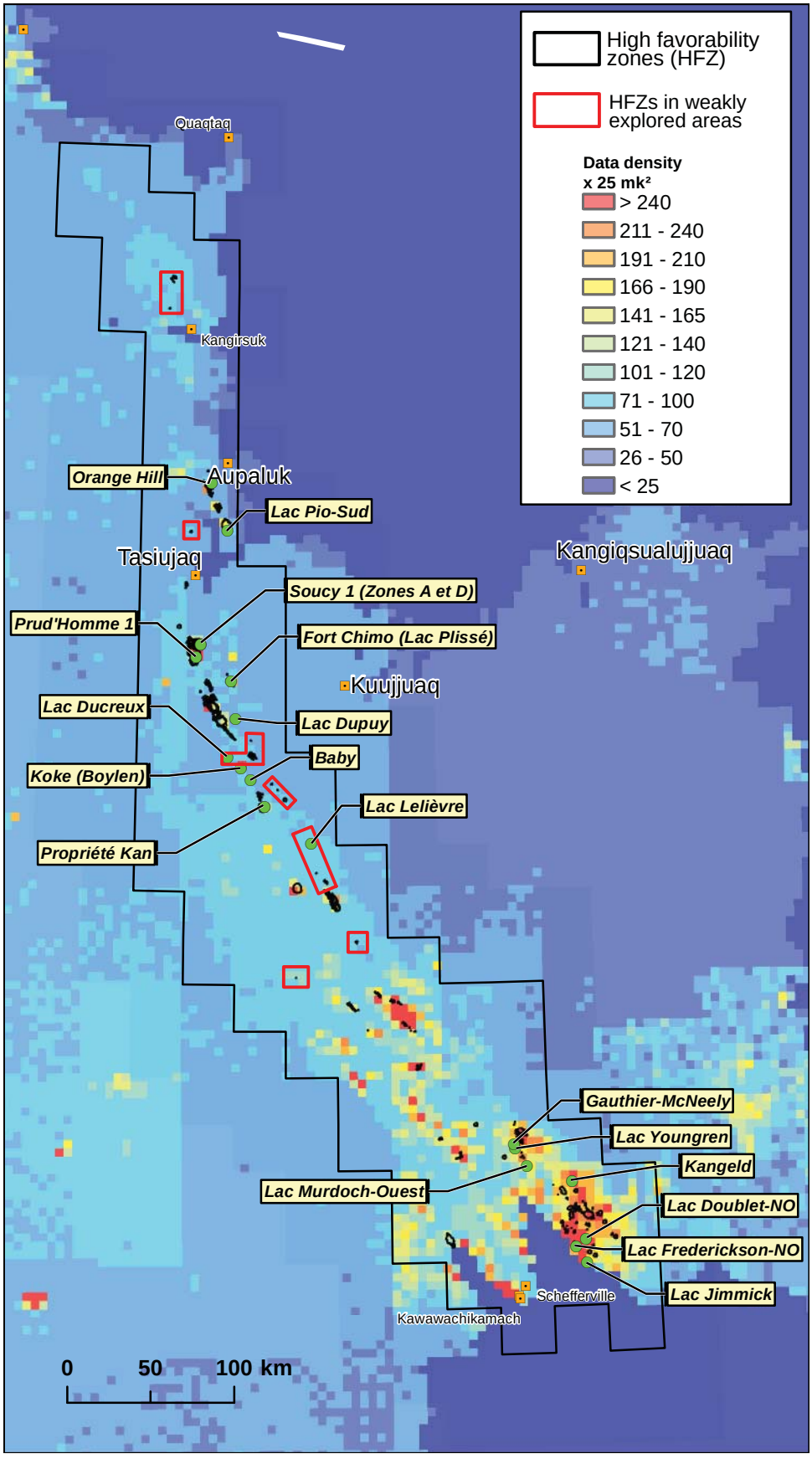


**FIGURE 18** – Location of HFZs according to the level of knowledge for the study area. Red polygons denote HFZs located in weakly explored areas where the potential to discover VMS deposits is favourable.

# RÉFÉRENCES


AGTERBERG, F.P., 1989 – Systematic approach to dealing with uncertainty of geoscience information in mineral exploration. Proceedings 21st APCOM Symposium, Las Vegas, march 1989; Chapter 18, pages 165-178.

AGTERBERG, F.P. – BONHAM-CARTER, G.F. – WRIGHT, D.F., 1990 – Statistical pattern integration for mineral exploration. *In*: Computer Applications in Resource Estimation Prediction and Assessment for Metals and Petroleum (Gaal, G. and Merriam, D.F., editors). Pergamon Press, Oxford; pages 1-21.

AN, P. – MOON, W.M. – RENCZ, A.N., 1991 – Application of fuzzy theory for integration of geological, geophysical and remotely sensed data. Canadian Journal of Exploration Geophysics; Volume 27, pages 1-11.

AN, P. – MOON, W.M. – BONHAM-CARTER, G.F., 1992 – On a knowledge-based approach of integrating remote sensing, geophysical and geological information. Proceedings IGARSS'92; pages 34-38.

BARAGAR, W.R.A., 1967 – Wakuach Lake map-area, Quebec-Labrador (23 O). Commission géologique de Canada, Mémoire 344, 174 pages.

BARAGAR, W.R.A. – SCOATES, R.F.J., 1981 – The circum-Superior belt : a Proterozoic plate margin? *In*: Precambrian Plate Tectonics (Kröner, A., editor). Developments in Precambrian Geology 4. Elsevier Scientific, Amsterdam; pages 297-330.

BARRETT, T.J. – WARES, R.P. – FOX, J.S., 1988 – Two-stage hydrothermal formation of a Lower Proterozoic sedimenthosted massive sulfide deposit, northern Labrador Trough, Quebec. Canadian Mineralogist; volume 26, pages 871-888.

BIRKETT, T.C. – CLARK, T., 1991 – Géologie et potentiel métallifère de la carbonatite protérozoïque du lac LeMoyne dans le nord du Québec. Commission géologique de Canada; Forum des travaux en cours, Programme et Résumés, page 20.

BOLENEUS, D.E. – RAINES, G.L. – CAUSEY, D. – BOOKSTROM, A.A. – FROST, T.P. – HYNDMAN, P.C., 2001 – Assessment method for epithermal gold deposits in northeast Washington State using weights-of-evidence GIS modelling. USGS; Open File report 01-501, 53 pages.

BONHAM-CARTER, G.F., 1994 – Geographic Information Systems for geoscientists: Modelling with GIS. Pergamon Press, Oxford; 398 pages.

BONHAM-CARTER, G.F. – AGTERBERG, F.P. – WRIGHT, D.F., 1988 – Integration of geological datasets for gold exploration in Nova Scotia. Photogrammetric Engineering and Remote Sensing; Volume 54, No.77, pages 1585-1592.

BONHAM-CARTER, G.F. – AGTERBERG, F.P. – WRIGHT, D.F., 1989 – Weights of evidence modelling: a new approach to mapping mineral potential. Statistical applications in the Earth Sciences; Geological Survey of Canada; Paper 89-9, pages 171-183.

BROWN, W. – GROVES, D.I. – GEDEON, T., 2003 – Use of fuzzy membership input layers to combine subjective geological knowledge and empirical data in a neural network method for mineral-potential mapping. Natural Resources Research; Volume 12, No.3, pages 183-200.

BROWN, W.M. – GEDEON, T.D. – GROVES, D.I. – BARNES, R.G., 2000 – Artificial neural networks; a new method for mineral prospectivity mapping. Australian Journal of Earth Sciences; Volume 47, No.4, pages 757-770.

CARRANZA, E.J.M. – HALE, M., 2002 – Where are Porphyry Copper Deposits Spatially localized? A case study in Benguet Province, Phillipines. Natural Resources Research; Volume 11, No. 1, pages 45-59.

Cheng, Q., 1999 – Spatial and scaling modelling for geochemical anomaly separation. Journal of Geochemical Exploration, Volume 65, pages 175-194.

Cheng, Q. – Agterberg, F.P. – Bonham-Carter, G.F., 1996. – A spatial analysis method for geochemical anomaly separation. Journal of Geochemical Exploration, Volume 56, pages 183-195.

Cheng, Q. – Agterberg, E P., 1999 – Fuzzy weights of evidence and its application in mineral potential mapping. Natural Resources Research; Volume 8, No. 1, pages 27-35.

Chung, C.F. – Agterberg, F.P., 1980 – Regression models for estimating mineral resources from geological map data. Mathematical Geology; Volume 12, No.5, pages 473-488.

Chung, C.F. – Moon, W.M., 1991 – Combination rules of spatial geoscience data for mineral exploration. Geoinformatics; Volume 2, pages 159-169.

Clark, T. – Thorpe, R.I., 1990 – Model lead ages from the Labrador Trough and their stratigraphic implications. *In*: The Early Proterozoic Trans-Hudson Orogen of North America : Lithotectonic Correlations and Evolution (Lewry, J.F. and Stauffer, M.R., editors). Geological Association of Canada; Special Paper 37, pages 413-432.

Clark, T. – Wares, R., 2004 – Synthèse lithotectonique et métallogénique de l'Orogène du Nouveau-Québec (Fosse du Labrador). Ministère des Ressources naturelles; MM 2004-01, 180 pages.

D'ercole, C. – Groves, D.I. – Knox-Robinson C.M., 2000 – Using fuzzy logic in a Geographic Information System environment to enhance conceptually based prospectivity analysis of Mississippi Valley-type mineralization. Australian Journal of Earth Sciences; Volume 47, pages 913-927.

de Araujo, C.C. – Macedo, A.B., 2002 – Multicriteria geologic data analysis for mineral favourability mapping: Application to a metal sulphide mineralized area, Ribeira Valley Metallogenic Province, Brazil. Natural Resources Research; Volume 11, No. 1, pages 29-43.

Dimroth, E., 1978 – Région de la Fosse du Labrador entre les latitudes 54° 30' et 56° 30'. Ministère des Ressources naturelles; RG 193, 412 pages.

Dimroth, E. – Baragar, W.R.A. – Bergeron, R. – Jackson, G.D. – 1970 – The filling of the Circum-Ungava geosyncline. *In*: Symposium on Basins and Geosynclines of the Canadian Shield (Baer, A.J., editor). Geological Survey of Canada; Paper 70-40, pages 45-142.

Dion, C. – Lamothe, D., 2002 – Évaluation du potentiel en minéralisations de sulfures massifs volcanogènes de la région de Chibougamau (32G) - Intégration de géodonnées par la technologie d'analyse spatiale. Ministère des Ressources naturelles; EP 2002-04, 1 cédérom.

Eckstrand, O.R. – Sinclair, W.D. – Thorpe, R.I., 1996 – Geology of Canadian Mineral Deposit Types, Decade in North American Geology, 8, Geological Survey of Canada. P-1, pages 129-196.

Findlay, J.M. – Parrish, R.R. – Birkett, T. – Watanabe, D.H., 1995 – U-Pb ages from the Nimish Formation and Montagnais glomeroporphyritic gabbro of the central New Québec Orogen, Canada. Canadian Journal of Earth Sciences; Volume 32, pages 1208-1220.

Franklin, J.M., 1995 – Volcanic-associated massive sulphide base metals. Geological Survey of Canada, Geology of Canada no.8, pages 158–183.

Franklin, J.M. – Gibson, H.L. – Jonasson, I.R. – Galley, A.G., 2005 – Volcanogenic Massive Sulfide Deposits. Society of Economic Geology; Economic Geology 100th Anniversary Volume; pages 523-560.

Frarey, M.J. – Duffell, S., 1964 – Revised stratigraphic nomenclature for the central part of the Labrador Trough. Geological Survey of Canada; Paper 64-25, 13 pages.

Galley, A.G., 1993 – Characteristics of semi-conformable alteration zones associated with volcanogenic massive sulphide districts. Journal of Geochemical Exploration; volume 48, pages 175–200.

Galley, A.G. – Hannington, M.D. – Jonasson, I.R., 2007 – Volcanogenic massive sulphide deposits. *In:* Mineral Deposits of Canada: A Synthesis of Major Deposit-Types, District Metal-

logeny, the Evolution of Geological Provinces, and Exploration Methods (Goodfellow, W.D., editor). Geological Association of Canada, Mineral Deposits Division; Special Publication No.5, pages 141-161.

Girard, R., 1990 – Les cisaillements latéraux dans l'arrière-pays des orogènes du Nouveau-Québec et de Torngat : une revue. Geoscience Canada; Volume 17, pages 301-304.

Goodfellow, W.D. – Zierenberg, R.A., – ODP 196 Shipboards Science Party, 1999 – Genesis of massive sulfide deposits at sediment-covered spreading centers. *In*: Volcanic-Associated Massive Sulfide Deposits: Processes and Examples in Modern and Ancient Settings (Barrie, C.T., and Hannington, M.D., editors). Reviews in Economic Geology; volume 8, Society of Economic Geologists, pages 297-324.

Groves, D.I. – Goldfarb, R.J. – Knox-Robinson, C.M. – Ojala, V.J. – Gardoll, S.J. – Yun G. Y. – Holyland P.W., 2000 – Late-kinematic timing of orogenic gold deposits and significance for computer based exploration techniques with emphasis on the Yilgarn Block, Western Australia. Ore Geology Reviews; Volume 17, pages 1-38.

Harris, J.R., 1989 – Data Integration for gold exploration in eastern Nova Scotia using a GIS. *In*: Proceedings of Remote Sensing for Exploration Geology, Calgary, Alberta. Published by Environmental Research Institute of Michigan; pages 233-249.

Harris, D.A. – Pan, R., 1999 – Mineral favourability mapping: a comparison of artificial networks, logistic regression and discriminant analysis. Natural Resources Research; Volume 8, No.2, pages 93-109.

Harris, J.R. – Sanborn-Barrie, M., 2006 – Mineral potential mapping : Examples from the Red Lake greenstone belt, northwest Ontario. *In*: GIS for the Earth Sciences (Harris, J.R., editor). Geological Association of Canada; Special Paper 44, pages 1-22.

Harris, J.R. – Wilkinson, L. – Broome, J., 1995 – Mineral exploration using GIS-based favourability analysis, Swayze Greenstone Belt, Northern Ontario. *In*: Proceedings of the Canadian Geomatics Conference (CD-ROM), National Defense Canada.

Harris, J.R. – Wilkinson, L. – Grunsky, E., 2000 – Effective use and interpretation of lithogeochemical data in regional mineral exploration programs: Application of Geographic Information System (GIS) technology. Ore Geology Reviews; Volume 16, pages 107-143.

Harris, J.R. – Wilkinson, L. – Grunsky, G. – Heather, K., Ayer, J., 1999 – Techniques for analysis and visualization of lithogeochemical data with applications to the Swayze greenstone belt, Ontario. Journal of Geochemical Exploration; Volume 67, No.1-3, pages 301-334.

Harris, J.R. – Wilkinson, L. – Heather, K. – Fumerton, S. – Bernier, M.A. – Ayer, J. – Dahn, R., 2001 – Application of GIS processing techniques for producing mineral prospectivity maps - A case study: Mesothermal Au in the Swayze greenstone belt, Ontario, Canada. Natural Resources Research; Volume 10, No.2, pages 91-124.

Hoffman, P., 1988 – United Plates of America, the birth of a Craton: Early Proterozoic assembly and growth of Proto-Laurentia. Annual Reviews of Earth and Planetary Sciences; Volume 16, pages 543-603.

Hoffman, P., 1989 – Precambrian geology and tectonic history of North America. In : The Geology of North America - An Overview (A.W. Bally and A.R. Palmer, editors). Geological Society of America, The Geology of North America; Volume A, pages 447-512.

Hoffman, P., 1990 – Dynamics of the tectonic assembly of northeast Laurentia in geon 18 (1.9-1.8 Ga). Geoscience Canada; Volume 17, pages 222-226.

Hoffman, P., – Grotzinger, J.P., 1989 – Abner-Denault reef complex (2.1 Ga), Labrador Trough, N.E. Québec. *In*: Reefs, Canada and Adjacent Area (Geldsetzer, H.H.J., James, N.P. and Tebbutt, G.E., editors). Canadian Society of Petroleum Geologists; Memoir 13, pages 49-54.

Ishikawa, Y. – Sawaguchi, T. – Iwaya, S. – Horiochi, M., 1976 – Delineation of prospecting targets for Kuroko deposits based on models of volcanism of underlying dacite and alteration halos: Mining Geology, 26, 105-117

James, D.T. – Dunning, G.R., 2000 – U-Pb geochronological constraints for Paleoproterozoic evolution of the Core Zone : southeastern Churchill Province, northeastern Laurentia. Precambrian Research; Volume 103, pages 31-54.

Knox-Robinson, C.M., 2000 – Vectorial fuzzy logic: a novel technique for enhanced mineral prospectivity mapping, with reference to the orogenic gold mineralization potential of the Kalgoorlie Terrane, Western Australia. Australian Journal of Earth Sciences; Volume 57, No. 5, pages 929-942.

Labbé, J.-Y., 2002 – Évaluation du potentiel de découverte de kimberlites de la région du Grand-Nord du Québec - Intégration de géodonnées par la technologie d'analyse spatiale. Ministère des Ressources naturelles; EP 2002-05, 1 cédérom.

Labbé, J.-Y. – Pilote, P. – Lamothe, D., 2006 – Évaluation du potentiel minéral pour les gîtes porphyriques de Cu-Au-Mo de l'Abitibi. Ministère des Ressources naturelles et de la Faune; EP 2006-03, 47 pages, 1 cédérom.

Lamothe, D., 2008 – Évaluation du potentiel en minéralisations de type or orogénique de la Baie James. Ministère des Ressources naturelles et de la Faune; EP 2008-01, 54 pages, 1 cédérom.

Lamothe, D., 2009 – Évaluation du potentiel minéral pour les gîtes porphyriques de Cu-Au ± Mo de la Baie James. Ministère des Ressources naturelles et de la Faune; EP 2009-01, 54 pages, 1 cédérom.

Lamothe, D., 2010 – Modélisation de cibles de l'environnement secondaire par des techniques de seuils naturels et de régression spatiale multiple. Ministère des Ressources naturelles et de la Faune; EP 2010-01, 28 pages, 1 cédérom.

Lamothe, D., 2011 – Potentiel en minéralisations de sulfures massifs volcanogènes de l'Abitibi – version 2011. Ministère des Ressources naturelles et de la Faune; EP 2011-01, 18 pages, 1 cédérom.

Lamothe, D. – Beaumier, M., 2001 – Évaluation du potentiel régional en minéralisations de type Olympic Dam-Kiruna dans la région du lac Manitou (SNRC 22I). Ministère des Ressources naturelles; EP 2001-01, 1 cédérom.

Lamothe, D. – Beaumier, M., 2002 – Évaluation du potentiel régional en minéralisations de type Olympic Dam-Kiruna dans la région du lac Fournier (SNRC 22P). Ministère des Ressources naturelles; EP 2002-01, 45 pages, 1 cédérom.

Lamothe, D. – Harris, J.R, 2006 – Évaluation du potentiel en minéralisations de type or orogénique des roches archéennes de l'Abitibi. Ministère des Ressources naturelles et de la Faune; EP 2006-01, 64 pages, 1 cédérom.

Lamothe, D. – Harris, J.R. – Labbé, J.-Y. – Doucet, P. – Houle, P. – Moorhead, J., 2005 – Évaluation du potentiel en minéralisations de type sulfures massifs volcanogènes (SMV) pour l'Abitibi. Ministère des Ressources naturelles, de la Faune et des Parcs; EP 2005-01, 99 pages, 1 cédérom.

Lydon, J. W., 1984 – Some observations on the morphology and ore textures of volcanogenic sulfide deposits of Cyprus. Geological Survey of Canada, Current Research, Paper 84-01A, pages 601-610.

Machado, N., 1990 – Timing of collisional events in the Trans-Hudson Orogen : evidence from U-Pb geochronology for the New Quebec Orogen, the Thompson Belt and the Reindeer Zone (Manitoba and Saskatchewan). *In*: The Early Proterozoic Trans-Hudson Orogen of North America : Lithotectonic Correlations and Evolution (Lewry, J.F. and Stauffer, M.R., editors). Geological Association of Canada; Special Paper 37, pages 433-441.

Machado, N. – Clark, T. – David, J. – Goulet, N., 1997 – U-Pb ages for magmatism and deformation in the New Quebec Orogen. Canadian Journal of Earth Sciences; Volume 34, pages 716-723.

Machado, N. – Goulet, N. – Gariépy, C., 1989 – U-Pb geochronology of reactivated Archean basement and of Hudsonian metamorphism in the northern Labrador Trough. Canadian Journal of Earth Sciences; Volume 26, pages 1-15.

Paganelli, F. – Richards, J.P. – Grunsky, E.C., 2002 – Integration of Structural, Gravity and Magnetic Data Using the Weights of Evidence Method as a tool for Kimberlite Exploration in the Buffalo Head Hills, Northern Central Alberta, Canada. Natural Resources Research; Volume 11, No. 3, pages 219-236.

Piché, M. – Jébrak, M., 2004 – Normative minerals and alteration indices developed for mineral exploration. Journal of Geochemical Exploration; Volume 82, pages 59-77.

Poirier, G. – Perreault, S. – Hynes, A., 1990 – The Nature of the eastern Boundary of the Labrador Trough Near Kuujjuaq, Quebec. *In*: The Early Proterozoic Trans-Hudson Orogen of North America : Lithotectonic Correlations and Evolution (Lewry, J.F. and Stauffer, M.R., editors). Geological Association of Canada; Special Paper 37, pages 397-412.

Porwal, A. – Carranza E.J.M. – Hale, M., 2003a – Artificial neural networks for mineral-potential mapping: A case study from the Aravalli Province, western India. Natural Resources Research; Volume 12, No. 3, pages 155-171.

Porwal, A. – Carranza E.J.M. – Hale, M., 2003b – Knowledge-driven and data-driven fuzzy modlels for predictive mineral potential mapping. Natural Resources Research; Volume 12, No. 1, pages 1-25.

Porwal, A. – Hale, M., 2000 – GIS-based weights-of-evidence analysis of multiclass spatial data for predictive mineral mapping: a case study from Aravalli province, western India: Proc. XIV Intern. Con. Applied Geologic Remote Sensing, (Las Vegas, Nevada); pages 377-384.

Raines, G.L., 1999 – Evaluation of Weights of Evidence to predict epithermal gold deposits in the Great Basin of the western United States. Natural Resources Research; Volume 8, No.4, pages 257-276.

Reddy, R.K.T. – Agterberg, F.P. – Bonham-Carter, G.F., 1991 – Application of GIS-based logistic models to base-metal potential mapping in Snow Lake area, Manitoba. *In*: Proceedings Canadian Conference on GIS, Ottawa, Canada, March 18-22, 1991; pages 607-618.

Rencz, A.N. – Harris, J.R. – Watson, G.P. – Murphy, B., 1994 – Data Integration for Mineral Exploration in the Antigonish Highlands, Nova Scotia. Canadian Journal of Remote Sensing; Volume 20, No.3, pages 258-267.

Rogge, D.M. – Halden, N.M. – Beaumont-Smith, C., 2006 – Application of Data Integration for Shear-Hosted Au Potential Modelling Linn Lake Greenstone Belt, Northwestern Manitoba, Canada. In: GIS for the Earth Sciences (Harris, J.R., editor). Geological Association of Canada; Special Paper 44, pages 191-210.

Rohon, M.-L. – Viallette, Y. – Clark, T. – Roger, G. – Ohnenstetter, D. – Vidal, P., 1993 – Aphebian mafic-ultramafic magmatism in the Labrador Trough (New Quebec): its age and the nature of its mantle source. Canadian Journal of Earth Sciences; Volume 30, pages 1582-1593.

Saeki, Y. – Date, J., 1980 – Computer applications to the alteration data of the footwall dacite lava at the Ezuri kuroko deposits, Akita Prefecture: Mining Geology, **30**, 4, 241-250.

Singer, D.A. – Kouda, R., 1996 – Application of feedforward neural network in search for Kuoroko deposits in the Hokuroku district, Japan. Mathematical Geology; Volume 28, No.3, pages 1017-1023.

Singer, D.A. – Kouda, R., 1997a – Use of a neural network to integrate geoscience information in the classification of mineral deposits and occurrences. *In:* Proceedings of Exploration 97: 4th Decennial International Conference on Mineral Exploration (Gubins, A.G., editor) pages 127-134.

Singer, D.A. – Kouda, R., 1997b – Classification of mineral deposits into types using mineralogy with a probabilistic neural network. Nonrenewable Resources; Volume 6, pages 27-32.

Singer, D.A. – Kouda, R., 1999 – A comparison of the weights-of-evidence method and probabilistic neural networks. Natural Resources Research; Volume 8, No. 4, pages 287-298.

Skulsky, T. – Wares, R.P. – Smith, A.D., 1993 – Early Proterozoic (1.88-1.87) tholeiitic magmatism in the New Québec Orogen. Canadian Journal of Earth Sciences; Volume 30, pages 1505-1520.

Spiegelhalter, D.J., 1986 – Uncertainty in expert systems. *In*: Artificial Intelligence and Statistics (Gale, W.A., editor). Addison-Wesley, Reading, Massachusetts; pages 17-25.

St. Seymour, K. – Kiddie, A. – Wares, R., 1991 – Basalts and gabbros of the Labrador Trough : remnants of a Proterozoic failed ocean? Neues Jahrbuch fuer Mineralogie, Monatshefte, 1991; Hefte 6, pages 271-280.

Stockwell, C.H., 1982 - Proposals for time classification and correlation of Precambrian rocks and events in Canada and adjacent areas of the Canadian Shield. Geological Survey of Canada; Study 80-19, 135 pages.

Tangestani, M.H. – Moore, F., 2003 – Mapping porphyry copper potential with a fuzzy model, northern Shar-e-Babak, Iran. Australian Journal of Earth Sciences; Volume 50, pages 311-317.

Trépanier, S., 2007 – Identification de domaines géochimiques à partir des levés régionaux de sédiments de lac. Ministère des Ressources naturelles, Québec; GM 62922, 95 pages.

Turner, D.D., 1997 – Predictive GIS Model for Sediment-Hosted Gold Deposits, North-Central Nevada, U.S.A. In: Proceedings of Exploration 97 : Fourth Decennial International Conference on Mineral Exploration (Gubins, A.G., editor). Exploration Information Management; Paper 13, pages 115-126.

Van der Leeden, J. – Bélanger, M. – Danis, D. – Girard, R. – Martelain, J., 1990 – Lithotectonic domains in the high-grade terrain east of the Labrador Trough (Quebec). *In*: The Early Proterozoic Trans-Hudson Orogen of North America (Lewry, J.F. and Stauffer, M.R., editors). Geological Association of Canada; Special Paper 37, pages 371-386.

Wardle, R.J. – James, D.T. – Scott, D.J. – Hall, J., 2002 – The southeastern Churchill Province : synthesis of a Paleoproterozoic transpressional orogen. Canadian Journal of Earth Sciences; Volume 9, pages 639-663.

WARDLE, R.J. – RYAN, B. – ERMANOVICS, I., 1990a – The eastern Churchill Province, Torngat and New Québec orogens : an overview. Geoscience Canada; Volume 17, pages 217-222.

WARDLE, R.J. – RYAN, B. – NUNN, G.A.G. – MENGEL, F.C., 1990b – Labrador segment of the Trans-Hudson orogen : crustal development through oblique convergence and collision. *In*: The Early Proterozoic Trans-Hudson Orogen of North America (Lewry, J.F. and Stauffer, M.R., editors). Geological Association of Canada; Special Paper 37, pages 353-369.

WARES, R., – BERGER, J. – ST. SEYMOUR, K., 1988 – Synthèse métallogénique des indices de sulfures au nord du 57e parallèle, Fosse du Labrador : Étape I. Ministère de l'Énergie et des Ressources, Québec; MB 88-05, 186 pages.

WILKINSON, L. – HARRIS, J.R. – KEATING, P. – KJARSGAARD, B., 2006 – GIS spatial analysis tools to assist in the search for kimberlite: Weights of evidence applied to the Lac de Gras region. In: GIS for the Earth Sciences (Harris, J.R., editor). Geological Association of Canada; Special Paper 44, pages 211-228.

WODICKA, N. – MADORE, L. – LARBI, Y. – VICKER, P., 2002 – Géochronologie U-Pb de filons-couches mafiques de la Ceinture de Cape Smith et de la Fosse du Labrador. Programme et résumés, 23e Séminaire d'information sur la recherche géologique. Ministère des Ressources naturelles, Québec; DV 2002-10, page 48.

WRIGHT, D.F., 1996 – Evaluating volcanic hosted massive sulphide favourability using GIS-based spatial data integration models, Snow Lake area, Manitoba. Unpublished Ph. D. thesis, University of Ottawa; 338 p.

WRIGHT, D.F. – BONHAM-CARTER, G.F., 1996 – VHMS Favourability Mapping with GIS-Based Integration Models, Chisel Lake-Anderson Lake Area. *In*: EXTECH I: A Multidisciplinary Approach to Massive Sulphide Research in the Rusty Lake- Snow Lake Greenstone Belts, Manitoba (Bonham-Carter, G.F., Galley, A.G., Hall, G.E.M., editors). Geological Survey of Canada; Bulletin 426, pages 339 -376 et 387-401.

# APPENDIX 1

Characteristics of the deposits used to calculate weight factors for the mineral potential map for mafic-pelitic-type VMS deposits (descriptions taken from Clark and Wares, 2004).

| DEPOSIT NAME | NTS | EASTING | NORTHING | DESCRIPTION | MULT. |
|---|---|---|---|---|---|
| Baby | 24F11 | 478736 | 6384165 | PY, PO in graphitic shales intercalated with carbonate and silicate iron formations and gabbros. | 1 |
| Fort Chimo (Lac Plissé) | 24K04 | 467168 | 6443164 | Massive and disseminated PO, CP, PY, SP in banded, cherty and carbonatized argillite near the contact with a gabbro; locally basalt | 2 |
| Gauthier-McNeely | 23O10 | 636421 | 6166954 | Disseminated to massive PO, SP, CP; concordant SF veins in conglomerates and graphitic argillites. | 2 |
| Kangeld | 23O08 | 671271 | 6144729 | PO and PY zone, massive and concordant, with disseminations, veinlets and stringers of CP, SP, GL, in graphitic and pyritic argillites. The SF are stratigraphically above a zone of sericite-chlorite schist and are overlain by basalts. | 2 |
| Koke (Boylen) | 24F11 | 473195 | 6391629 | Massive, stratiform SF, concordant with stratification, in a graphitic slate (with associated basalt) near the summit of an iron formation. The SF consist of PY, SP, GL, PO and CP, in a groundmass of chert and very fine-grained carbonate. They contain beds and fragments of chert and fragments of dolomite. The deposit is highly deformed and located in the core of an isoclinal syncline (F1 fold) refolded by open to tight F2 folds. | 3 |
| Lac Doublet-NW | 23O01 | 679496 | 6110478 | Semi-massive and disseminated SF (CP, PO) in slate and disseminated SF in basalt and along pillow margins. Mineralization is strongest near the contact with the slate. | 1 |
| Lac Ducreux | 24F12 | 465232 | 6398060 | Massive PO, PY (laminations, nodules) in a silicate iron formation with chert beds; disseminated PY in QZ veins cutting graphitic shale and sericite schist. | 2 |
| Lac Dupuy | 24F13 | 470045 | 6420729 | Massive SF (PO, PY, CP, SP) in black shale at the contact with a gabbro. | 1 |
| Lac Frederickson-NW | 23O01 | 673596 | 6105629 | Several concordant lenses of semi-massive SF (CP, PO, SP, PY, GL), in cherty argillites of the Menihek Formation and bordered by gabbro sills. | 3 |
| Lac Jimmick | 23J16 | 680121 | 6096129 | SP, CP in greywackes and fractured carbonatized mudstones. | 3 |
| Lac Lelièvre | 24F07 | 515145 | 6346229 | Disseminated PY, PO, CP in gabbro (undetermined type); massive PY, PO in lenses and disseminated syngenetic PY, PO in metasediments; epigenetic veins of massive PY, PO and disseminated SP, CP cutting the metasediments. | 2 |
| Lac Murdoch-Ouest | 23O10 | 644045 | 6153729 | Lens of massive SF (50% PO, 50% CP) in a thin horizon of argillaceous schist (+siltstone, quartzite, greywacke), between a glomeroporphyritic gabbro and an aphyric gabbro (small showing). | 1 |
| Lac Pio-Sud (HR96-3293) | 24K13 | 464991 | 6533567 | Disseminated CP in a PO-rich iron formation. | 1 |
| Lac Youngren | 23O10 | 637045 | 6164028 | Veinlets of QZ-FP-CB and PO-CP-SP cross-cutting or parallel to bedding, over a distance of more than 12 m, in quartzites and argillites near a contact with fine-grained gabbro; locally fine-grained PO. Several drill holes intersected Cu-, Zn-, Au-, Ag-rich sections of limited size. | 2 |
| Orange Hill | 24N04 | 455804 | 6561878 | Massive SF, 1 metre thick (unknown length), in an iron formation. | 1 |
| Kan property | 24F06 | 487195 | 6368379 | Lens of massive SF (PY, PO, GL, SP) traceable over 40 m (N-S) in carbonatized shales (graphitic phyllite) in contact with a sericitic and carbonatized schist (metabasalt) and carbonate iron formation; presence of graphitic shale beds. Alteration of nearby basalts: CB, AK, SR, CL (phyllites and schists). The massive SF occur in a mineralized horizon (disseminated sulphides) 3 m thick and traceable for 400 m to the north. The deposit appears to occur in the nose of a minor syncline plunging to the southeast. | 2 |
| Prud'Homme No. 1: South Zone | 24K05 | 446596 | 6457930 | South Zone: lens of massive SF (PO, CP, SP, traces GL) oriented NNW-SSE and measuring 180 m x 55 m, in sheared contact with a gabbro; presence of framboidal PY; 5 to 10% gangue composed of iron-CB, QZ, SE, GN, SR. North Zone: a series of masses and lenses of massive SF (PY, PO, CP, SP, trace GL) in CB, CL, QZ schists bordered by gabbros; the mineralized zone is oriented N-S and measures 200 to 300 m long with decametre-scale thicknesses. | 3 |
| Soucy No. 1 (A and D zones) | 24K05 | 449053 | 6465574 | A Zone: massive SF (PY, PO, CP, SP, GL), concordant, in QZ-CC gangue, 400 m long with a maximum thickness of 40 m (drill holes); very fine SF in a black schist; framboidal PY. D Zone: PY, PO, CP, SP, concordant deposit at least 130 m long with a maximum thickness of 10 m (drill holes), in a black shale. | 3 |

The 18 deposits are located on Figure 8. The weight factor calculation for each parameter was assessed using a set of mineral occurences representing known VMS deposits in the region. The set was weighted according to the importance of each deposit. Showings are represented by single occurences, worked deposits by two superimposed occurences, and deposits with tonnage estimates by three superimposed occurences. The description of each deposit is from Clark and Wares (2004).

# APPENDIX 2

Favourability assessment for each parameter used in the processing

| *Unit or Distance (m)* | Contrast | Fuzzy value | Rank |
|---|---|---|---|
| **Lithological control** | | | |
| **Favourable stratigraphic unit** | | | |
| Middle Baby Formation (iron formation: carbonate and silico-carbonate facies, chert interbeds) | 5.749 | 0.799 | 17 |
| Lower Baby Formation (black pyritic slate, pyritic siltstone) | 5.728 | 0.798 | |
| Hellancourt Formation (massive basalt) | 3.481 | 0.681 | |
| Upper Baby Formation (rhythmites: mudstone, siltstone, fine sandstone) | 3.118 | 0.662 | |
| Menihek Formation (mudstone, siltstone, phyllite and slatey schist with minor amounts of sandstone) | 2.027 | 0.605 | |
| Willbob Formation | 1.897 | 0.599 | |
| Hellancourt Formation (basalt, some tuff and breccia) | 0.448 | 0.523 | |
| Other units | -3.425 | 0.295 | |
| **Proximity to an intrusion of the Montagnais Suite** | | | |
| 0 | 1.261 | 0.566 | 22 |
| 0 - 200 | 2.884 | 0.650 | |
| > 200 | -2.755 | 0.335 | |
| **Presence of breccias** | | | |
| < 200 | 6.992 | 0.864 | 9 |
| 200 - 1200 | 3.523 | 0.683 | |
| 1200 - 2600 | 3.366 | 0.675 | |
| > 2600 | -3.999 | 0.260 | |
| **Evidences of hydrothermal activities** | | | |
| **Alteration minerals** | | | |
| **Anomalous Hashimoto index** | | | |
| < 400 | 5.121 | 0.766 | 19 |
| 400 - 2200 | 1.504 | 0.578 | |
| > 2200 | -2.474 | 0.352 | |
| **Sericite anomal index** | | | |
| < 400 | 5.841 | 0.804 | 16 |
| > 400 | -5.841 | 0.150 | |
| **ISER anomal index** | | | |
| < 600 | 4.987 | 0.759 | 20 |
| > 600 | -4.987 | 0.201 | |
| **IFRAIS anomal index** | | | |
| < 400 | 5.238 | 0.772 | 18 |
| > 400 | -5.238 | 0.186 | |
| **Alteration minerals** | | | |
| **Proximity to carbonate alteration** | | | |
| < 200 | 6.712 | 0.849 | 13 |
| 200 - 400 | 6.076 | 0.816 | |
| 400 - 2800 | 2.037 | 0.606 | |
| > 2800 | -3.164 | 0.310 | |
| **Proximity to iron alteration** | | | |
| < 200 | 8.094 | 0.921 | 6 |
| 200 - 1400 | 3.177 | 0.665 | |
| 1400 - 2800 | 0.629 | 0.533 | |
| > 2800 | -3.601 | 0.284 | |
| **Presence of graphite** | | | |
| < 200 | 6.928 | 0.860 | 11 |
| 200 - 400 | 3.588 | 0.687 | |
| > 400 | -5.889 | 0.147 | |
| **Presence of sulfures or oxydes** | | | |
| **Presence of pyrite** | | | |
| < 200 | 6.839 | 0.856 | 12 |
| 200 - 800 | 2.923 | 0.652 | |
| 800 - 2000 | 2.307 | 0.620 | |
| > 2000 | -3.829 | 0.271 | |
| **Presence of pyrrhotite** | | | |
| < 200 | 7.813 | 0.906 | 7 |
| 200 - 600 | 2.908 | 0.651 | |
| 600 - 1000 | 2.955 | 0.654 | |
| 1000 - 1600 | 2.367 | 0.623 | |
| 1600 - 2400 | 1.446 | 0.575 | |
| > 2400 | -4.816 | 0.211 | |
| **Presence of chalcopyrite** | | | |
| < 200 | 8.327 | 0.933 | 5 |
| 200 - 2000 | 2.698 | 0.640 | |
| > 2000 | -4.600 | 0.224 | |
| **Presence of sphalérite** | | | |
| < 800 | 8.343 | 0.934 | 4 |
| > 800 | -8.343 | 0.001 | |
| **Presence of magnétite** | | | |
| < 200 | 4.547 | 0.736 | 21 |
| 200 - 1000 | 2.374 | 0.623 | |
| > 1000 | -3.056 | 0.317 | |

***Unit or Distance*** = Name of the favourable unit or the distance class used; ***Contrast*** = predictivity as calculated by WofE; **Fuzzy value** = Value obtained by transforming the contrast value into a fuzzy value; **Rank** = order of parameter favourability.

# APPENDIX 2

Favourability assessment for each parameter used in the processing (concluded)

| *Unit or Distance (m)* | Contrast | Fuzzy value | Rank |
|---|---|---|---|
| **Evidences of hydrothermal activities (suite)** | | | |
| **Indicator metals** | | | |
| **Anomalous copper content** | | | |
| < 500 | 6.940 | 0.861 | 10 |
| 500 - 2500 | 0.857 | 0.545 | |
| > 2500 | -3.932 | 0.264 | |
| **Anomalous zinc content** | | | |
| < 400 | 8.585 | 0.950 | 3 |
| 400 - 1000 | 4.268 | 0.722 | |
| 1000 - 2800 | 1.251 | 0.565 | |
| > 2800 | -4.788 | 0.213 | |
| **Anomalous lead content** | | | |
| < 400 | 9.615 | 0.999 | 1 |
| 400 - 1000 | 4.801 | 0.750 | |
| > 1000 | -4.833 | 0.210 | |
| **Anomalous cobalt content** | | | |
| < 400 | 7.294 | 0.879 | 8 |
| > 400 | -4.336 | 0.240 | |
| **Anomalous silver content** | | | |
| < 400 | 6.073 | 0.816 | 15 |
| 400 - 2800 | 2.548 | 0.632 | |
| > 2800 | -4.152 | 0.251 | |
| **Anomalous gold content** | | | |
| < 200 | 9.118 | 0.974 | 2 |
| 200 - 400 | 7.015 | 0.865 | |
| 400 - 600 | 5.136 | 0.767 | |
| 600 - 800 | 4.818 | 0.751 | |
| 800 - 2800 | 1.025 | 0.553 | |
| > 2800 | -4.397 | 0.237 | |
| **Anomalous manganese content** | | | |
| < 200 | 6.521 | 0.839 | 14 |
| 200 - 400 | 5.378 | 0.780 | |
| > 400 | -3.838 | 0.270 | |
| **Secondary environnement** | | | |
| **Anomalous copper in lake sediments** | | | |
| 0 - 1000 | 1.995 | 0.604 | 25 |
| 1000 - 3500 | 1.350 | 0.570 | |
| > 3500 | -1.551 | 0.407 | |
| **Anomalous zinc in lake sediments** | | | |
| 0 - 1000 | 2.261 | 0.618 | 24 |
| 1000 - 2500 | 1.538 | 0.580 | |
| 2500 - 4000 | 1.112 | 0.558 | |
| > 4000 | -1.805 | 0.392 | |
| **Anomalous cobalt in lake sediments** | | | |
| 0 - 1000 | 2.743 | 0.643 | 23 |
| 1000 - 2000 | 1.153 | 0.560 | |
| 2000 - 4000 | 0.877 | 0.546 | |
| > 4000 | -1.554 | 0.407 | |

***Unit or Distance*** = Name of the favourable unit or the distance class used; ***Contrast*** = predictivity as calculated by WofE; **Fuzzy value** = Value obtained by transforming the contrast value into a fuzzy value; **Rank** = order of parameter favourability.

# APPENDIX 3

Inference model for pelitic-mafic-type VMS mineral potential in the Labrador Trough

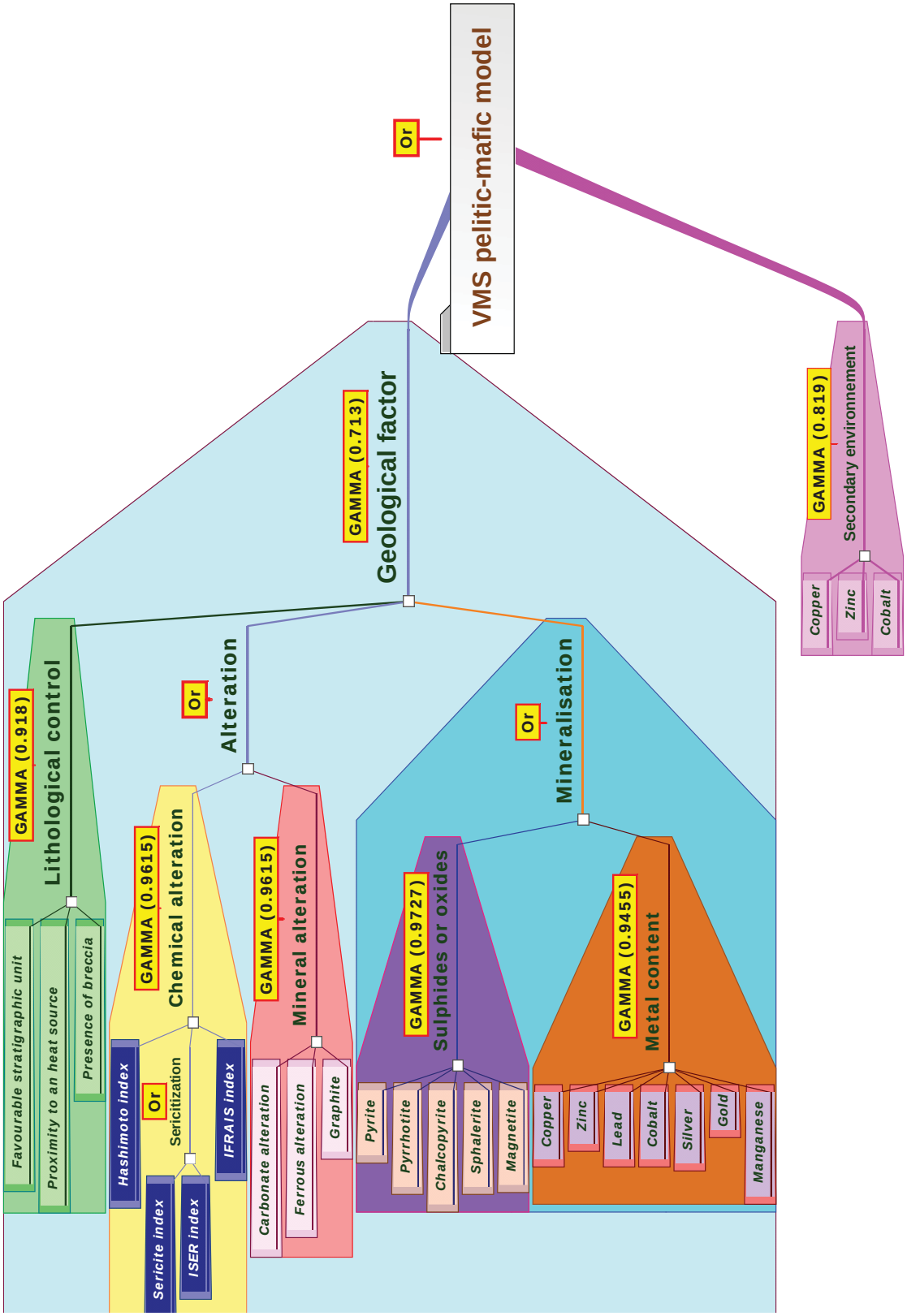


This inference model illustrates the process for combining the 25 geological parameters used in the processing. The parameters, as well as the subsets, were all combined using fuzzy logic operators. Numbers in parentheses after each FUZZYGAMMA operator represent the factor used to calibrate the subset so as to obtain a background value of about 0.5 on the final map.

*Ressources naturelles*
Québec